



Internal thermal mass for passive cooling and ventilation: adaptive comfort limits, ideal quantities, embodied carbon

SPECIAL COLLECTION:
ALTERNATIVES TO
AIR CONDITIONING:
POLICIES, DESIGN,
TECHNOLOGIES,
BEHAVIOURS

RESEARCH

TIMOTHÉE DE TOLDI

SALMAAN CRAIG

LAXMI SUSHAMA

*Author affiliations can be found in the back matter of this article

]U[ubiquity press

ABSTRACT

How effective is naturally ventilated internal thermal mass for obviating air-conditioning, mitigating heatwaves and storing carbon in buildings? This study combines detailed climate model outputs with scaling rules for optimizing internal thermal mass coupled with buoyancy ventilation. It identifies regions where this passive design strategy is most effective during future heatwaves and determines how much internal thermal mass each person needs to stay comfortable in these regions, with a special focus on Canada. Results suggest that naturally ventilated internal thermal mass is likely to become less effective due to future global heating. Regions where internal thermal mass will no longer be sufficient to obviate air-conditioning and where it can still play a significant role in hybrid cooling are identified. By comparing the ideal per capita thermal mass quantities in different regions, it is found that biomass-based materials require approximately 3.5 times the volume of cementitious materials to perform equivalently, if thermal proportions for surface area and thickness are respected. Finally, an analysis of the per capita embodied carbon of these ideal internal thermal mass quantities is undertaken, suggesting a fair functional unit to compare thermal mass materials.

PRACTICE RELEVANCE

High-resolution Canadian maps and lower-resolution global maps are developed in this study to allow practitioners to distinguish between areas where internal thermal mass should be sufficient to obviate air-conditioning and where supplementary cooling is needed. Ideal per capita quantities of different thermal mass materials are given for each region, with guidelines for how to distribute this thermal mass internally in walls, floors and ceilings, and how the surface area and thickness of the thermal mass scales with the thermal properties of the material and the per capita heat loads and ventilation and temperature damping requirements. As such, this study suggests how thermal mass materials can be compared fairly in terms of performance and embodied carbon at the preliminary stages of design.

CORRESPONDING AUTHOR:

Timothée de Toldi

Civil Engineering, McGill
University, Montreal, QC,
Canada

timothee.detoldi@mail.mcgill.ca

KEYWORDS:

building design; cooling; cooling technologies; demographics; energy use; environmental impacts; passive cooling; standards; thermal mass

TO CITE THIS ARTICLE:

De Toldi, T., Craig, S., & Sushama, L. (2022). Internal thermal mass for passive cooling and ventilation: adaptive comfort limits, ideal quantities, embodied carbon. *Buildings and Cities*, 3(1), pp. 42–67. DOI: <https://doi.org/10.5334/bc.156>

1. INTRODUCTION

The global energy demand for cooling represents 10% of all global electricity consumption today and is expected to triple by 2050, with a corresponding increase in refrigerant leakage (IEA 2018). It is therefore essential to revisit and develop alternatives to standard air-conditioning and to understand their limits in a warming world. ‘Sustainable cooling’ (Khosla et al. 2021: 3) refers to the:

provisions of cooling that minimize health impacts from extreme heat [while] reducing greenhouse gas (GHG) emissions and [...] societal inequalities.

Khosla et al. (2021) identify five interconnected levers capable of driving sustainable system change for cooling, three of which imply more thoughtful and integrated approaches to architectural design: technology innovation, including energy-efficient and affordable passive and active cooling; infrastructure design, such as space design that predetermines cooling demand; and social interactions, such as the role of lifestyles and behavior on cooling demand.

There has been a shift of emphasis recently from focusing mainly on energy efficiency as a way to reduce the operational impacts of buildings towards a recognition that reducing the upfront and end-of-life emissions of construction is also critically important (Hoxha et al. 2020; Pomponi & Moncaster 2016; Pomponi et al. 2016; Röck et al. 2020). Although several voluntary initiatives exist for embodied carbon accounting (Pomponi et al. 2018), mandatory policies regarding embodied carbon in the construction sector are uncommon, mostly due to the following obstacles:

- a lack of a standardized methodology for embodied carbon accounting (De Wolf et al. 2017; Moncaster et al. 2018)
- systemic spatial and temporal accounting discrepancies exacerbated by the hardly traceable global material geography of multilayered product assemblies (Habert et al. 2020; Lützkendorf 2020) and the wide variety of actors concerned (manufacturers, contractors, investors, designers, etc.) and
- the complex and volatile aspects of defining baseline scenarios for comparative lifecycle assessment (LCA) analyses (Carlisle et al. 2021; Harmon 2019).

There is general agreement that new and retrofitted buildings should be conceived to meet strict embodied and operational emission cuts, and new approaches should be devised to assess and predict their environmental impact with more confidence while allowing design teams to fairly compare the various options available to them. Yet, systemic assessments of the effectiveness, performance and adequacy of passive cooling approaches in a warming climate are lacking. One problem is the disconnect between building simulations and global climate models (GCMs). Building performance simulations require high-resolution hourly data. However, both the GCMs and regional climate models (RCMs; i.e. dynamic downscaling simulations of GCMs outputs), which are used to understand climate behavior and to project probable changes (Knutti et al. 2013), typically lack the necessary temporal/spatial resolution that building simulations require (Yassaghi & Hoque 2019). RCM outputs have been further downscaled to obtain high-resolution data, using statistical (statistical downscaling models) or dynamic (convection-permitting models) approaches (Moazami et al. 2019) to bridge the gaps between building and climate science and to evaluate regional-scale projections of changes in certain variables, such as cooling loads (Berardi & Jafarpur 2020). Yet studies that use RCMs and GCMs to qualitatively evaluate the applicability of passive cooling measures as part of integrated, scalable design approaches are few and far between.

One fundamental method for passive cooling is using the building structure as thermal mass and coupling it with natural ventilation. Uninsulated thermal mass has been used to buffer external temperature variations to regulate the internal temperature of buildings for centuries (Addis 2007). This kind of approach, where the thermal mass has a direct thermal connection between inside and outside, can be highly effective for passive cooling when the average daily temperature is thermally comfortable (i.e. acceptable for the intended use). However, very few regions around the world have, or will have, such an ideal climate year-round. Externally insulating the thermal mass is therefore necessary in most instances, for when heating or cooling must be added

internally. However, this presents a challenge for passive cooling during opportune times when the building can be operated in free-running mode. How to discharge the internal thermal mass at night of the heat it has accumulated during the day? One approach is night ventilation, and it is possible to design the building so this discharging process occurs naturally in the absence of both wind and fans. Holford & Woods (2007) showed how to size an internal thermal mass so that it powers a natural cycle of buoyancy (*i.e.* thermally driven) ventilation over 24 h. This approach ensures that the building is adequately ventilated and the thermal mass discharges sufficiently at night, even when there is no wind. Their analysis was further developed by characterizing how changes to internal heat loads and wind loads affected the evolution of internal temperatures (Lishman & Woods 2009). More recently, the optimal quantities and proportions of an internal thermal mass were defined for any target temperature damping and natural ventilation rate in a simple harmonic cycle (Craig 2019). Small-scale experiments suggest that the natural coupling of internal thermal mass and buoyancy ventilation evolves predictably, according to these scaling rules and design guidelines (Barrett et al. 2021).

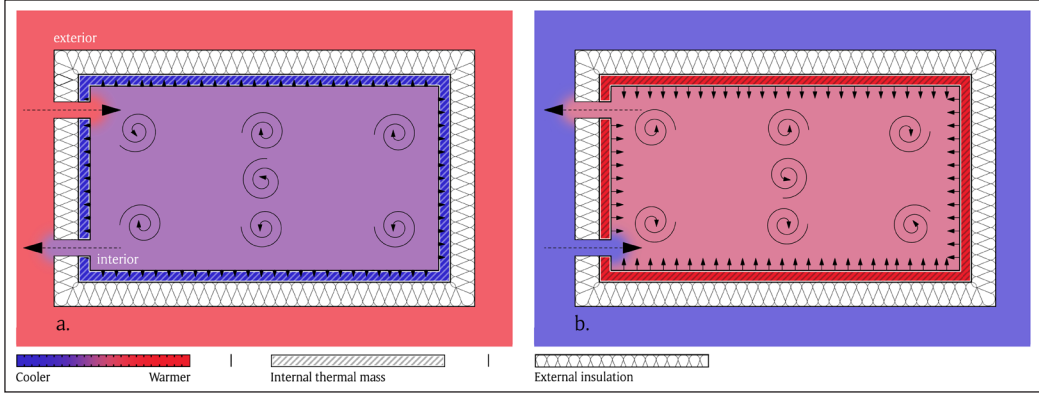
This study investigates the potential of naturally ventilated internal thermal mass as a strategy for obviating air-conditioning and reducing embodied carbon in different regions of a heating world. The emphasis given to the Canadian context stems from the relevance of this approach in North American temperate and subpolar climates. On the one hand, very cold temperatures during long Canadian winters require building envelopes to meet strict airtightness and insulation standards (NRC 2010). On the other hand, summer cooling loads are expected to increase by 31% on average in the next 30–50 years (Berardi & Jafarpur 2020), due to exacerbated urban heat island effects (Roberge & Sushama 2018) and predicted increases in heatwave frequency and magnitude (ECCC 2018–21), as testified by the Western North America summer 2021 heatwave where Canadian temperatures of up to 49.6°C were recorded (ECCC 2021). Another opportunity that this passive cooling approach presents in Canada and other regions is the potential link between construction materials and natural climate solutions, *i.e.* the protection, management and restoration of natural systems. One recent study identified and evaluated 24 natural climate solutions in Canada, three of which could eventually lead to a sustainable stream of carbon-storing construction materials at the regional scale: the use of crop residues, the use of winter cover crops and better forest management (Drever et al. 2021). Examining the limits of carbon storage in construction materials at the regional level, within the sustainable capacity of ecosystems services, is crucial in light of the climate emergency. For instance, one study examining bio-based insulation materials for retrofitting the Portuguese building stock highlighted the potential of straw-based insulation, not only because fast-growing biomass can sequester more carbon but also because of the current status and capacity of agricultural landscapes in Europe (Göswein et al. 2021).

The present study estimates the per capita quantities of naturally ventilated internal thermal mass required to avoid air-conditioning in Canada and other regions around the world, and the carbon emissions associated with these quantities of thermal mass materials. The ideal quantities of concrete, timber and straw-based composites are defined in a scalable way to fairly represent key differences between cementitious materials, harvested wood products (HWPs) and fast-growing bio-based materials. High-resolution RCM outputs (average daily temperature swings during the 30 consecutive hottest days in every location) are extracted to estimate, for every 50 × 50 km grid cell over Canada, the local interior temperature damping necessary to meet adaptive comfort standards during future heatwaves. Local levels of temperature damping requirements are correlated with required internal thermal mass proportions using thermal mass scaling rules (Craig 2019). As the methodology is meant to be extended to other regions, indicative results are provided on a global scale using lower resolution GCM outputs.

2. COUPLING OF INTERNAL THERMAL MASS AND NATURAL VENTILATION

Prior to describing the methodology, the purpose of this section is to describe the model for naturally ventilated internal thermal mass which underpins the analysis.

2.1 NATURALLY VENTILATED INTERNAL THERMAL MASS MODEL



The relationship between *internal thermal mass* and *buoyancy-driven ventilation* is well characterized (Holford & Woods 2007). Buoyancy ventilation refers to the practice of configuring a space and its openings to spontaneously drive airflow by interior-exterior temperature differentials. The model described by Holford & Woods (2007), which assumes an interior space connected to the exterior only by a lower and an upper ventilation opening, harnesses natural feedback cycles driven by the daily swing of exterior temperature for interior thermoregulation. The internal thermal mass is coupled to the exterior temperature oscillations not through the envelope but by thermally driven (*i.e.* buoyancy) ventilation. This is the natural mechanism by which the internal thermal mass charges during the day and discharges at night (**Figure 1**). During the night, the thermal mass is relatively warm compared with the exterior, so it heats up the interior air, which exhausts upwards (**Figure 1**, scenario b). During the day, the thermal mass is relatively cool compared with the exterior, so it cools down the interior air, which exhausts downwards (**Figure 1**, scenario a).

The thermal relationships between heat diffusion in the thermal mass, natural convection at the surface of the thermal mass, and buoyancy ventilation exchange between the interior and exterior are parametrized in terms of dimensionless ratios (Holford & Woods 2007). The global behavior is controlled by two non-dimensional parameters: the massing parameter (Ω) and the ventilation parameter (F). The massing parameter Ω describes the ratio of thermal storage to surface heat transfer and thus controls the heat exchanges driven by the thermal mass as it heats and cools. It is defined as:

$$\Omega = \frac{\omega \rho c l l_r}{h \lambda} \quad (1)$$

where h is the surface heat transfer coefficient ($\text{W}/\text{m}^2\cdot\text{K}$); ρc is the volumetric heat capacity of the thermal mass; $\omega = 2\pi/86400$ is the angular frequency; l_r is the fraction of material thickness needed for the lumped mass to do the equivalent work of the entire mass thickness (l); and λ is a factor that determines the surface temperature by approximating the temperature gradients inside the mass, respectively defined as:

$$l_r = \frac{\cosh(2\eta) - \cos(2\eta)}{\eta(\sinh(2\eta) + \sin(2\eta))} \quad (2)$$

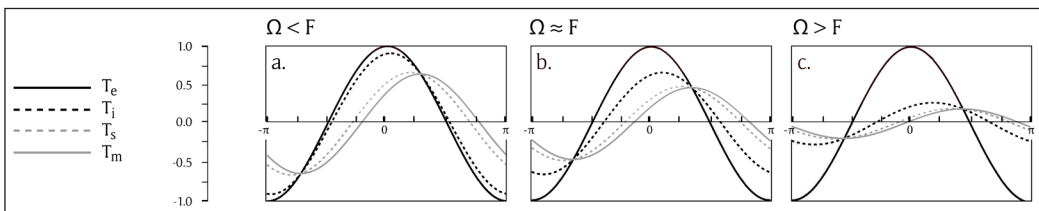


Figure 1: Vertical section of a well-mixed interior space with naturally ventilated internal thermal mass. Heat is transferred between the interior air and the environment via the ventilation flow (dashed arrows), and between the interior air and the thermal mass by convection (solid arrows). Scenarios a: daytime (thermal mass charging by buoyancy ventilation); and scenario b: night-time (thermal mass discharging by buoyancy ventilation).

Figure 2: Influence of the thermal mass (Ω) and ventilation (F) parameters over interior (T_i), thermal mass (T_m) and thermal mass surface (T_s) temperatures, driven by the cyclic changes in the external temperature (T_e) over a period of $2\pi = 24$ h.

$$\lambda = 1 / \left(1 + \left(\frac{\eta(\sinh(2\eta)) + \sin(2\eta)}{\xi(\cosh(2\eta) - \cos(2\eta))} \right) \right) \quad (3)$$

where η is the ratio of the layer thickness to the depth of thermal penetration; and ξ is the potential rate of heat storage compared with the rate of surface heat transfer, both functions of thermal properties of the mass. Finally, F , which compares the ventilation heat transfer with the surface heat transfer and thus translates the relative heat exchanges in which the ventilation can partake, is defined as follows:

$$F = \frac{Q \rho_i c_i}{Sh} \quad (4)$$

where $\rho_i c_i$ is the volumetric heat capacity of air ($1.23 \times 10^3 \text{ J/m}^3/\text{K}$); and Q is the rate of ventilation (m^3/s), computed as follows:

$$Q = A^* \sqrt{\beta g H |T_e - T_i|} \quad (5)$$

where T_e and T_i are the exterior and interior temperatures; and β is the thermal expansion coefficient of air. When $\Omega > F$, the thermal mass dominates, i.e. the air changes are relatively low and the interior temperature is highly damped (**Figure 2**, scenario c). When $F > \Omega$, the ventilation dominates: the air changes are relatively high, and the thermal mass hardly affects the interior temperature (**Figure 2**, scenario a).

2.2 NATURALLY VENTILATED INTERNAL THERMAL MASS MODEL LIMITATIONS

It is important to emphasize three simplifying assumptions built into the Holford & Woods (2007) model. First, the model assumes a simple harmonic cycle (i.e. a repeating thermal history with no lag effects from prior days). Second, the model assumes negligible conduction heat transfer between the thermal mass and the exterior. In other words, the thermal mass is connected to the exterior temperature oscillations by thermally driven ventilation exchanges only. Third, the model assumes no additional heat gains or losses (e.g. from people, equipment, solar radiation, conduction from other parts of the envelope, etc.). The effect of changing internal heat loads and wind loads on the evolution of internal temperatures in this configuration has been studied (Lishman & Woods 2009), but is not considered in the present analysis.

Despite these simplifications, recent experiments show that the natural coupling of internal thermal mass and buoyancy ventilation evolves as expected, suggesting this internal mass model can predict the free-running temperatures and ventilation rates quite reliably (Barrett et al. 2021). However, it is important to check that the heat transfer at the inner surface of the internal thermal mass (h_S) will be greater than the heat transfer through the external envelope (U_A ; W/K). This assumption ($h_S \gg U_A$) is easily respected for most typical modern building assemblies, i.e. insulated by materials with U -values < 0.2 . The effect of conduction gains/losses and other heat gains/losses can be estimated by adding or subtracting heat from the ventilation stream before it enters the building, thus addressing the limitations of the third assumption (see the methodology subsequently developed in Subsection 3.1.3 below).

2.3 NORMALIZED DAMPING

Traditional continuous thermal mass assemblies are typically thick enough to produce temperature lag effects that can last several days, allowing interior spaces to be cooled below the exterior daily mean temperature during hotter days. The cooling capacity of naturally ventilated internal thermal mass in harmonic cycles (i.e. assuming no lag effects from prior days) can at best lower the interior maximum daily temperature to the exterior daily mean temperature (tending towards **Figure 2**, scenario c) (Holford & Woods 2007). This damping effect, M , is defined as the ratio of the interior temperature damping, i.e. the difference between the maximum daily exterior ($T_{e_{\max}}$) and interior ($T_{i_{\max}}$) temperature, to the exterior daily temperature increments above the mean temperature ($T_{e_{\text{mean}}}$):

where M can be measured in idealized terms, so that the essential thermodynamic behavior of internal thermal mass is defined relative to the minimum (-1) and maximum (1) normalized exterior temperature in a daily cycle (**Figure 3**), where time is expressed in radians (1 h = $2\pi/24$). When internal thermal mass hardly affects the interior conditions, which are thus almost identical to the exterior ones, M gets closer to 0 (**Figure 3**, scenario a). Alternately, when interior conditions are highly damped by the work of internal thermal mass, M gets closer to 1 (**Figure 3**, scenario c). The work of internal thermal mass driven by natural continuous feedback cycles is therefore limited by exterior temperature oscillations (e.g. the exterior daily mean temperature), and, as corroborated by recent empirical evidence (i.e. live testing chambers) (Barrett et al. 2021), the thermodynamic limit of naturally ventilated internal thermal mass passive cooling thus translates as $M = 1$.

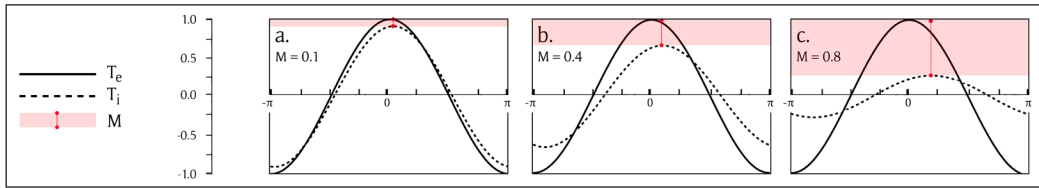


Figure 3: Cyclic changes in the exterior (T_e) and interior (T_i) temperatures over a period of $2\pi = 24$ h, with corresponding temperature damping coefficients (M).

2.4 OPTIMAL TUNING OF NATURALLY VENTILATED INTERNAL THERMAL MASS

To achieve controlled temperature differentials between exterior and interior, the thermal mass (Ω) and ventilation (F) parameters are optimized. The optimal pairing allows an optimization of the delay in heat transfer from the mass to its surface to account for a specified maximum interior-exterior temperature differential (i.e. the desired temperature damping) expressed in terms of temperature damping coefficients (M). The optimal pairings (**Figure 4**) are numerically solved (Craig 2019) for each increment of M by simultaneously solving the following equations:

$$M = 1 - \frac{\sqrt{1 + \Omega^2}}{\sqrt{1 + \left[\Omega + 1.07 \left(\frac{\lambda^2}{F^2 \Omega^2} \right)^{\frac{1}{3}} \Omega \right]^2}} \quad (7)$$

$$\left(\frac{F}{\lambda} \right)_{\max} = \tan \left(\frac{1.07}{2} * \Omega^{\frac{4}{3}} \right) - 1 \quad (8)$$

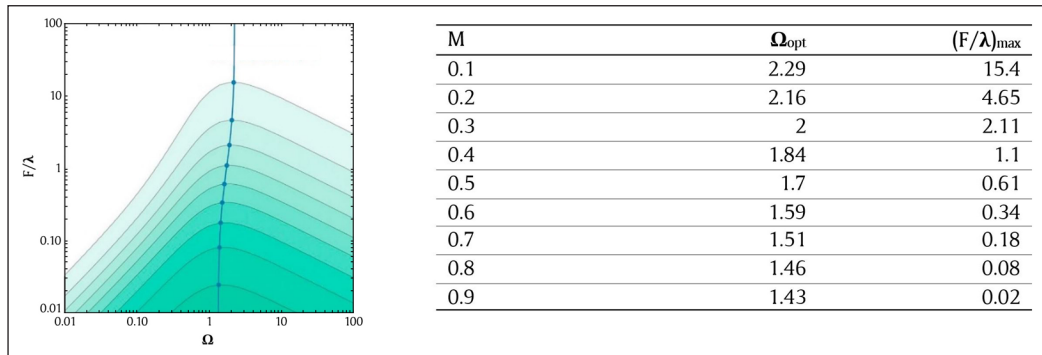


Figure 4: Optimal pairing (blue curve) of massing parameter (Ω) and ventilation parameter (F/λ) for every increment of temperature damping coefficient (M).

The pairings can then be used to solve for the optimal ratios that give the balance of dimensions needed to keep the thermal exchanges optimally synchronized in space. These ratios will be referred to as *scaling rules*. The optimal thickness (l ; cm) of the material and the resulting temperature delay (λ ; dimensionless) are then solved for each increment of M by simultaneously solving

equations (1) to (3), while the optimal surface of thermal mass internally exposed (S ; m^2) (see equation 4) is computed for any desired ventilation rate (Q ; m^3/s). Recent experiments validated, for several materials (i.e. biogenic and cementitious) and climates, the reasonable accuracy with which the scaling rules can predict the interior temperature damping and ventilation flow rates of spaces whose thermal mass is designed (thickness and surface area) to meet specific targets (Barrett et al. 2021).

3. METHOD

The subsequent methodology consists of three parts, respectively covering the parametrization of the adaptive comfort limits of naturally ventilated internal thermal mass (which will subsequently be referred to as thermal mass), the ideal per person quantities of materials required to meet such standards, and the embodied carbon emissions of such material quantities.

3.1 ADAPTIVE COMFORT LIMITS

Where in Canada, and more generally in the world, might thermal mass be sufficient for all cooling needs now and in the future? Does its effectiveness decrease with climate change? This section presents the theoretical framework and data used to establish the heatwave-mitigation potential of internal thermal mass.

3.1.1 Adaptive comfort and effectiveness of naturally ventilated internal thermal mass

The shift toward a lower carbon society has created a new context for comfort, from it being considered a ‘product’ delivered by energy-intensive machines with a conventional emphasis on uniformity to a broader notion that takes into consideration adaptive behaviors (Brager et al. 2015; Cole et al. 2008; Nicol 2006; Nicol et al. 2012). Research has shown that what occupants deemed comfortable in naturally ventilated buildings varied depending on local climates (ANSI/ASHRAE 2017). In this regard, regions are identified according to the ability of naturally ventilated internal thermal mass to dampen interior conditions enough to meet neutral adaptive comfort interior air temperatures (T_n) during the hottest month of the year. ASHRAE’s Standard 55 (ANSI/ASHRAE 2017) defines the upper 80% acceptability limit of interior neutral air temperature inside of naturally ventilated buildings as a function of the monthly mean air temperature ($T_{e\text{mean}}$):

$$T_n = 0.31 T_{e\text{mean}} + 21.3 \quad (9)$$

To define where thermal mass passive cooling is effective, and where it is not, four levels of effectiveness, relative to the physical limits of thermal mass and adaptive comfort thresholds, are defined. The levels are defined using the damping effect M required to meet adaptive comfort standards during the hottest month. While $M = 1$ represents the thermodynamic upper limit of a thermal mass in a repeating harmonic cycle, M is allowed to run higher to show hierarchy in regions where thermal mass could not provide all the cooling required during the hottest month. The percentage of sensible cooling loads (SCL; %), which internal thermal mass can provide for, can thus be expressed as follows:

$$SCL(\%) = \frac{1}{M} * 100\% \quad (10)$$

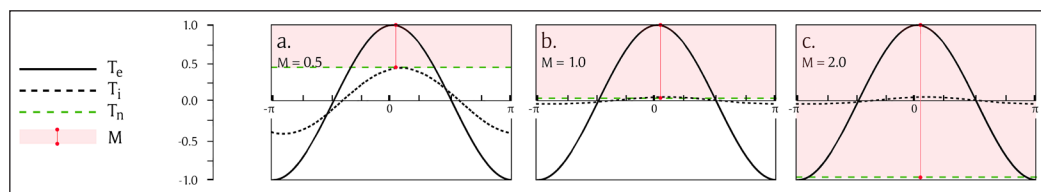


Figure 5 illustrates three scenarios that depict the correlation between exterior temperature oscillations and interior neutral temperature levels. In scenario a, providing sufficient thermal

Figure 5: Damping coefficient (M) required to meet adaptive comfort neutral temperature (T_n), within thermal mass thermodynamic capacity (scenarios a and b, with $M \leq 1$), or beyond thermal mass thermodynamic limit (scenario c, with $M \geq 1$).

comfort is within the thermodynamic capacity of internal thermal mass: the neutral temperature is higher than the exterior mean temperature; the required damping coefficient to meet that neutral temperature during the hottest time of the day is 0.5; thermal mass could provide for 200% of SCL (i.e. twice the required cooling). Conversely, in scenario c, the neutral temperature is lower than the exterior mean temperature; the damping coefficient required to meet such levels during the hottest time of the day is 2; thermal mass can only provide for 50% of SCL (i.e. half the required cooling). The thermal mass effectiveness levels are subsequently defined as follows:

- *Unnecessary*

Regions where $M < 0.2$, little to no cooling is required during the hottest month, and thus thermal mass is of no use.

- *Effective*

Regions where $0.2 < M < 1$, thermal mass could provide all the sensible cooling required to meet adaptive comfort during the hottest months, and thus obviate the use of mechanical air-conditioning.

- *Partially effective*

Regions where $1 < M < 2$, thermal mass could provide more than half the sensible cooling required to meet adaptive comfort during the hottest months. While supplementary cooling is therefore necessary for these regions during the hottest month, thermal mass could scale down air-conditioning energy consumption.

- *Ineffective*

Regions where $M > 2$, thermal mass could only provide less than half the sensible cooling required to meet adaptive comfort during the hottest months. A different form of cooling is therefore required in these regions.

ASHRAE's Standard 55 (ANSI/ASHRAE 2017) provides interior neutral temperatures in naturally ventilated buildings for exterior monthly mean temperatures of up to 33.5°C, setting the endpoint of interior adaptive comfort temperatures at 31.68°C (see equation 9). As the study requires a continuous index to be developed across all regions, the interior neutral temperature associated with exterior monthly mean temperatures $> 33.5^\circ\text{C}$ is thus set to 31.68°C.

While cooling is most often required for comfort, it may also be required for safety in cases of extreme compound temperature and relative humidity events (Sherwood & Huber 2010). Adaptive comfort standards generally discard humidity levels, and the correlated latent loads (ANSI/ASHRAE 2017; Manu et al. 2016), because non-negligible biophysical heat stress is assumed to happen at temperature levels above the endpoints of adaptive comfort models (Sadeghi et al. 2021). Trying to address and bridge the correlations and discrepancies between adaptive comfort models and safety thresholds is beyond the scope of this study, which thus discards the influence of relative humidity levels and interior latent loads.

3.1.2 Data from regional and global climate models (GCMs and RCMs)

The methodology developed here allows for regions to be classified based on adaptive comfort thresholds and is first illustrated through a case study of the Canadian territories. To that end, high-resolution outputs from RCM simulations over Canada are used. Like GCMs, RCMs are complex mathematical parametrizations of the interactions between major climate system components (mainly atmosphere, land surface, ocean, sea ice and vegetation), whose behaviors under forced changes (e.g. increased atmospheric greenhouse gas (GHG) concentration) are studied to understand their impact on climate. RCM simulations work by dynamically downscaling GCM data (used as boundary conditions) over selected regions, increasing both the simulation's resolution and accuracy. In this study, outputs from the Global Environmental Multi-Scale (GEM) RCM model (Côté et al. 1998), whose ability to simulate climate characteristics over Canada has been demonstrated (Teufel & Sushama 2019), are used to constitute climate data representative of Canada's current climate (1975–2005) and future climate projections (2055–85). Two different future climate scenarios corresponding to different representative concentration pathways (RCPs) are considered, i.e. RCP 4.5 and 8.5, which correspond to intermediate and high emission scenarios,

respectively. The data used are extracted from GEM model simulations that downscale CanESM2 GCM data (i.e. GCM data developed by Environment and Climate Change Canada for global climate analyses; Government of Canada 2021) over Canada at a 50 km resolution.

Adaptive comfort standards define the neutral temperature as a function of the mean monthly temperature. To identify regions according to the adaptive comfort thresholds, the average daily mean and maximum 2 m air temperature of the yearly rolling 30 hottest days (respectively $T_{e_{\text{mean}}}$ and $T_{e_{\text{max}}}$) are thus extracted from the RCM outputs and averaged over the periods considered. These variables are then used to compute local magnitudes of M as follows:

$$M = \frac{T_{e_{\text{max}}} - T_n}{T_{e_{\text{max}}} - T_{e_{\text{mean}}}} \quad (11)$$

The methodology can be extended to other world regions. Lower resolution indicative results are provided in a global analysis, useful for a high-level identification of regions with a high potential for thermal mass passive cooling, to guide the focus of subsequent regional studies. To that end, several GCM outputs are used to constitute a multi-model average representative of the current global climate (2005–25) and future global climate projections (2055–85, with RCP 2.6, 4.5 and 8.5 scenarios). GCMs differ in their respective responses to changing atmospheric GHG concentrations (IPCC 2021), and they can be classified according to their equilibrium climate sensitivity, referring to the amount of global surface warming that will occur in response to a doubling of atmospheric CO₂ concentrations. Three GCMs are used to constitute the multi-model average outputs used in the global analysis; the MRI-CGCM3, the CanESM2 and the HadGEM2-ES, with, respectively, low, medium and high equilibrium climate sensitivities (2.6, 3.7 and 4.6°C, respectively). These models are selected from the fifth phase of the Coupled Model Intercomparison Project (CMIP5) (a multi-model dataset coordinated by the World Climate Research Program), and their simulations have been validated and found to transcribe historical and present-day global climate characteristics well (Lee et al. 2015). The same method as outlined above for the regional analysis is used for the lower resolution global analysis: adaptive comfort thresholds are computed by extracting the average daily mean and maximum 2 m air temperature of the yearly rolling 30 hottest days in every GCM grid cell.

A sensitivity analysis was conducted using the yearly 10-day hottest windows for high-concentration pathways (RCP 4.5 and 8.5 scenarios) and found the transcribed global cooling needs are on average 12.9% higher than when computed using 30-day windows, only reasonably affecting the global repartition of thermal mass effectiveness levels.

The properties of the RCM and GCMs used in the analysis are listed in **Table 1**.

Table 1: Properties of selected regional and global climate models.

REGIONAL CLIMATE MODEL (RCM)	GRID CELL RESOLUTION (KM)	INPUT BOUNDARY CONDITION
Global Environmental Multi-Scale (GEM)	50 × 50	CanESM2
GLOBAL CLIMATE MODELS (GCMS)		
MRI-CGCM3	≈ 125 × 125	2.6
CanESM2	≈ 310 × 310	3.7
HadGEM2-ES	≈ 140 × 210	4.6

3.1.3 Ventilation rates and heat loads

Standards for healthy indoor thermal environments and air quality prescribe various per person-required ventilation rates (Q), based on the occupancy type of buildings (Khovalyg et al. 2020), which vary from 4 to 10 L/s. A conservative estimate of $Q = 10$ L/s per person is assumed in this study to consistently comply with building norms.

Realistic interior conditions comprise heat sources of different sizes that are unharmoniously synchronized in time. These interior heat loads, such as bodies or electrical appliances, tend to diminish or disappear at night. During their peak, they can significantly heat the interior air and

the exposed thermal mass surfaces by convection and radiation. The approach is to account for interior heat loads (H) by artificially raising the temperature of the air vented in at a rate of 10 L/s per person. H is assumed to be discontinuous, with a peak ventilation heating of 100 W, which accounts for 75 W per person of sensible heat gain (the per person loads for moderately active office work/standing/walking) and an additional 25 W for electrical appliances (this corresponds, for instance, to conservative estimates for a computer in energy saver mode) (ASHRAE 2013). Note that electrical loads tend to be shared among people. The mean and maximum exterior air temperatures (Te_{mean} and Te_{max} , respectively) are thus raised to compute the mean and maximum effective incoming air temperatures (Tei_{mean} and Tei_{max}) in the following manner:

$$Tei_{\text{mean}} = Te_{\text{mean}} + \left(\frac{H}{Qc_i \rho_i} * \frac{1}{2} \right) \quad (12)$$

$$Tei_{\text{max}} = Te_{\text{max}} + \frac{H}{Qc_i \rho_i} \quad (13)$$

where $\rho_i c_i$ is the volumetric heat capacity of air ($1.23 \times 10^3 \text{ J/m}^3/\text{K}$); and Tei_{mean} and Tei_{max} are then, respectively, substituted to Te_{mean} and Te_{max} in the computing of local magnitudes of M (see equation 11). **Figure 6** shows how the internal heat load assumption influences the temperature signal of the air vented in.

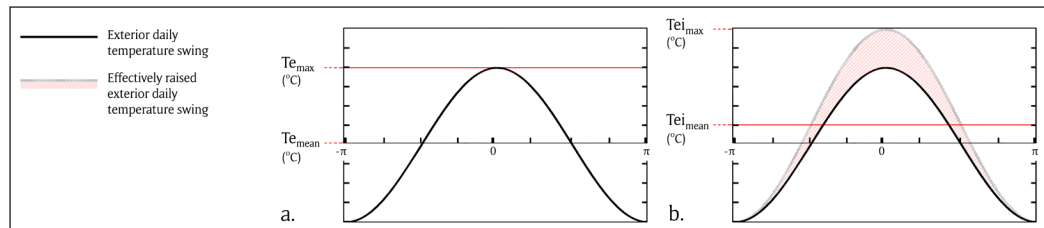


Figure 6: Exterior daily temperature swings (a) with corresponding mean and maximum daily exterior temperatures (Te_{mean} and Te_{max} , respectively), and effectively increased exterior daily temperature swing (b) with corresponding mean and maximum effective incoming air temperatures (Tei_{mean} and Tei_{max}) over a period of $2\pi = 24$ h.

3.2 IDEAL QUANTITIES

How much material is needed, on a per capita basis, to harness the maximum achievable potential of thermal mass? How can biogenic building materials be scaled to work as well as traditional thermal mass materials, such as concrete? This section determines the per person thermal mass material quantities required to provide thermal comfort during the hottest month without mechanical assistance in thermal mass-friendly climates. These quantities should be understood as the volumes of material required for per person inhabited floor space.

3.2.1 Thermal mass materials

Three representative material candidates are selected to compare the performance of both fast versus slow rotation biomass-based materials, and biomass-based materials versus traditional cementitious materials.

Mass-timber-based materials, i.e. softwood HWPs, are selected as representative slow-rotation biomass-based materials. HWPs can take the form of cross, glue, nail and dowel laminated timber. They are widely available in Canada (Head et al. 2019, 2020) from managed forest ecosystems (226 million ha, 750 000 ha of which are harvested every year, for a yearly average harvest volume of 158 million m³; Statistics Canada 2018).

Wheat-straw-based materials are then considered in the form of oriented straw structural boards (OSSBs). With 9.5 million ha of seeded areas (Statistics Canada 2021), wheat is the most cultivated fast-rotation plant in Canada, and wheat straw is a direct byproduct of its exploitation. On average, 52% of the straw produced in Canadian provinces remains available after cattle and soil conservation requirements (PPG & TCIC 2008), a varying proportion of which is incinerated or landfilled. With an estimated 4.59 tons per ha of seeded area (ADEME & IGN 2019), attributing 10% of the straw available on the Canadian market every year to the production of straw boards

would provide a continuous yearly supply of 2.78–3.70 million m³ of straw boards (assuming a conservative density of 600–800 kg/m³; Tabarsa et al. 2011).

Finally, concretes are considered as reference cementitious materials with higher thermal inertia, i.e. higher thermal conductivity and diffusivity.

MATERIAL	CONDUCTIVITY κ (W/M.K)	VOLUMETRIC HEAT CAPACITY ρC (MJ/m ³ /K)	SOURCES
Concrete	1.60 ± 0.80	2.28 ± 0.44	Ashby (2011)
Mass timber (softwood)	0.19 ± 0.11	0.85 ± 0.27	Ashby (2013)
Wheat straw OSSB	0.21 ± 0.02	1.02 ± 0.15	Cheng et al. (2013); Igaz et al. (2017); Tabarsa et al. (2011)

Representative ranges of thermal properties for each of these materials are outlined in **Table 2**. Mass timber properties are selected to account for a wide range of softwood species, with densities ranging from 440 to 600 kg/m³. The uncertainty ranges of HWP's thermal properties are also a function of the ambient conditions, as well as the direction and location of measurements: the thermal properties of samples used in construction projects should directly be measured for specific accuracy. The selected thermal properties of OSSB correspond to relatively dense panels, with densities ranging from 600 to 800 kg/m³. While the use of straw fibers allows the production of panels over a large range of densities, typically ranging from 200 to 800 kg/m³ (Tabarsa et al. 2011), it is assumed that the production or selection of OSSB panels purposed to act as thermal mass would likely target higher ranges of thermal inertia.

Table 2: Representative range of thermal properties for selected thermal mass materials.

Note: OSSB = oriented straw structural board.

3.2.2 Heat transfer coefficient

The heat transfer coefficient (h) used in the internal thermal mass model (see equations 1 and 4) is a quantitative characteristic summing the convective and radiative heat transfer (h_c and h_r , respectively) between the thermal mass surface and the surrounding air, and must fairly represent the heat transfer at the surface of the thermal mass. For this purpose, a typical space typology is defined. The authors assume a physical scenario where long, insulated interior spaces have thermal mass on one side, but not on the opposite side. The thermal mass is assumed to be vertically exposed on 3 m-high wall surfaces (standard floor-to-ceiling height). The heat transfer coefficient is estimated from the effective incoming air mean rolling temperature Tei_{mean} (i.e. the mean rolling exterior temperature adjusted to account for interior heat loads) and from the average effective incoming air temperature increment above the mean ($\Delta Tei = |Tei_{max} - Tei_{mean}|$) of the yearly hottest 30-day window averaged over the 2055–85 period:

$$h = h_c + h_r \quad (14)$$

$$h_r = \epsilon \sigma 4 (Tei_{mean} + (\Delta Tei / 2))^3 \quad (15)$$

$$h_c = \frac{Nu * \kappa}{L} \quad (16)$$

where κ is the thermal conductivity of the fluid (in this case, air); $\epsilon = 0.8$; σ is the Stefan–Boltzmann constant; Nu is a weighted average of the laminar and turbulent Nusselt numbers (Nu_l and Nu_t , respectively) computed with standard empirical correlations (Nellis & Klein 2009) not shown here; and L is the height of the vertical wall (i.e. 3 m). Using the Tei_{mean} and ΔTei averages and standard deviations (32.25 ± 1.86 and 6.35 ± 2.97°C, respectively) (**Figure 13**) from the global analysis for all RCP scenarios over thermal mass-friendly climates (i.e. where thermal mass is effective or partially effective), a sensible universal heat transfer coefficient range is found to be 7.38 ± 0.56 W/m².K (**Figure 7**). For comparison, exclusively Canadian data give a similar range of 7.91 ± 0.50 W/m².K.

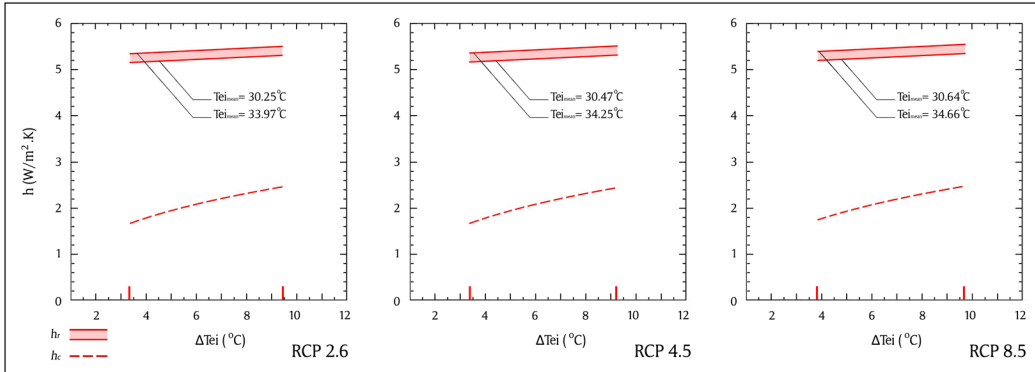


Figure 7: Universal estimates of radiant and convective heat transfer coefficients (h_r and h_c , respectively) shown to be similar for the RCP 2.6, 4.5 and 8.5 scenarios.

3.2.3 Per person material requirements

The optimal pairings of the thermal mass (Ω) and ventilation (F) parameters provided by Craig (2019), and the universal heat transfer coefficient range are used to compute the optimal thickness (l ; cm) of thermal mass (and the resulting temperature delay, λ) for each material type and for each increment of M (within the thermodynamic limit of thermal mass, i.e. $0.0 < M < 1.0$) by simultaneously solving equations (1) to (3). The optimal per person material surface (S ; m²) is then computed (see equation 4) using conservative per person ventilation rates, i.e. $Q = 0.01 \text{ m}^3/\text{s}$ (Khovalyg et al. 2020). The per person optimal thermal mass thickness and surface are multiplied to obtain the per person material volume (V ; m³).

A sensitivity analysis performed using a heat transfer coefficient range that accounts for vertical wall heights (L) of 2–4 m shows the negligible influence of L on the per person material requirements; volumes of material are found to differ only by 0.019% on average with $L = 2$ m, and by 0.044% with $L = 4$ m.

Using the per person required volumes of concrete for each increment of M as a reference scenario, material substitution factors (S_f) are developed, reflecting the quantities of materials—in volumetric units—required to perform equivalently to concrete.

3.3 EMBODIED CARBON

Typical inter-material comparative LCAs compare the embodied emission of equivalent volumes of materials, discarding the variability of the volumes required to perform the same function from one material to another and thus introducing significant sources of uncertainty in the results. Recent studies of the Canadian building industry have underlined the necessity to develop functional units from substitution factors developed at regional scales to increase the robustness of comparative LCAs and guide actors of the building sector towards environmentally coherent material selections in the early stages of design (Cordier et al. 2021). This section shows how the embodied carbon emissions of material volumes with equivalent thermal performance could be compared on a per capita basis to allow fair material comparisons. As embodied carbon data are by nature region specific (e.g. forestry ecosystems, manufacturing specificities, etc.), this study uses the Canadian framework as an illustrative case study. Data gathering and computation details are outlined in Appendices 2 and 3 in the supplemental data online.

3.3.1 Functional unit

To compare the environmental impact and the climate mitigation potential of various materials, the study defines and relies on a fair functional unit. The latter corresponds to the per person material requirements (V) needed to provide the temperature damping M necessary for thermal comfort during the hottest month without mechanical assistance, assuming that the material is ideally distributed as internal thermal mass, the natural ventilation rate is 10 L/s per person and the internal gains are 100 W per person (see Subsection 3.2). Subsequent sections show how this functional unit could be incorporated into current typical LCA practices. In this section, the lifecycle stages are described according to the EN 15804 standard (CEN 2011).

3.3.2 Inter-material comparative LCA

de Toldi et al.
Buildings and Cities
DOI: 10.5334/bc.156

54

Conventional inter-material comparative LCA practices primarily rely on the comparison of cradle-to-gate embodied emissions (Lützkendorf 2020), i.e. corresponding to the A1–A3 material life stages (raw material supply, transport to manufacturing site and manufacturing), collected for each material in the form of environmental product declarations (EPDs), which typically provide emission data for a specific volume of material (e.g. 1 m³) in a global warming potential format (GWP; kg CO₂,eq). While this approach is limited by its externalities (i.e. discarding the dynamic emissions associated with other/later life-stages, such as later carbonation for concrete, or carbon uptake and sequestration for biomass-based materials), EPDs remain the most available carbon emission data format to practitioners of the building industry for product comparison and procurement decisions (Waldman et al. 2020). The incorporation of every life stage discarded from EPDs is beyond the scope of this study (which aims to provide a replicable methodology); an illustrative use of the substitution factor-based functional unit is thus conducted relying solely on EPDs. Strictly Canadian EPDs are collected using the EC3 database (EC3 2020). The latter uses a methodology that quantitatively accounts for estimates of variation in underlying data specificity to compute the embodied emission uncertainty range associated with each EPDs (Waldman et al. 2020). The resulting high end of the uncertainty range for each EPD is then taken to generate conservative to achievable GWP estimates for each material (i.e. respectively, 80% and 20% of the EPDs indicating a GWP below this value).

4. RESULTS

The subsequent results are divided into three parts. The first part shows the effectiveness of thermal mass to provide adaptive comfort in future heatwaves throughout Canada without mechanical cooling assistance. Indicative results are also provided on a global scale to identify other regions with a high potential for applicability. The second part shows the ideal per person quantities of thermal mass required to meet adaptive comfort standards. The third part shows the lifecycle carbon emissions associated with these quantities of materials. Detailed tables of the per person quantities and associated lifecycle carbon emissions are provided in Appendix 1 in the supplemental data online.

4.1 ADAPTIVE COMFORT LIMITS

4.1.1 Naturally ventilated internal thermal mass limits for adaptive comfort in Canada

The effectiveness of thermal mass in Canada is shown in [Figure 8](#) for present and future climates. The color scales indicate regions where thermal mass is unnecessary (white), effective (green), partially effective (amber) and ineffective (grey) to meet adaptive comfort standards during the yearly 30-day hottest window.

The results suggest three visible trends. First, virtually all the Canadian population (close to 99% in every scenario) is shown to reside in climates where cooling is necessary during the hottest month of the year. Second, wherever cooling is necessary, thermal mass is shown to be useful (i.e. effective or partially effective), and able to cut significant portions of SCL (50–100%). This is shown by the absence of climates where thermal mass is ‘ineffective’ (i.e. indicated in grey), regardless of the future climate scenario considered. Yet, third, the effectiveness of thermal mass is shown to decrease due to future global heating; regions where thermal mass is deemed ‘effective’ are shown to be pushed further north, while regions where thermal mass is deemed only ‘partially effective’ are shown to drastically extend in future climates, i.e. they more than double in the RCP 4.5 scenario (+125.6%) and triple in the RCP 8.5 scenario (+197.8%). Further studies should analyze the aptitude for coupling good thermal mass design to other passive cooling strategies to evaluate the local potentials for air-conditioning substitution in the regions where thermal mass is ‘partially effective’, in which strategic harnessing of plural passive cooling methods might still allow full replacement of mechanical systems.

Altogether, the results suggest that while the number of buildings that can entirely rely on thermal mass for cooling requirements will decrease in Canada, thermal mass could still play a significant role in hybrid cooling approaches, regardless of the future climate scenario considered.

4.1.2 Naturally ventilated internal thermal mass limits for adaptive comfort in the world

Indicative results of the effectiveness of naturally ventilated internal thermal mass on a global scale are shown in **Figures 10** and **11** for present and future climates, while the rate of change of thermal mass effectiveness in future climates is shown in **Figure 12**. The population data (Jones & O'Neill 2016) used in future projections (**Figure 9**) account for changes (e.g. growths and migrations) according to the emission scenario considered. Population projections from the shared socioeconomic pathways (SSPs) 1, 2 and 5 are used for the RCP 2.6, 4.5 and 8.5 scenarios, respectively, due to their approximative correspondence (Meinshausen et al. 2020).

The results suggest that the extent of climates where thermal mass can currently answer all sensible cooling needs is, on a global scale, rather limited. **Figures 9a** and **10a** show that in the last two decades, about one-tenth (10.3%) of the world's population lived in climates where thermal mass and natural ventilation was sufficient for all cooling needs during the yearly hottest 30 consecutive days, and thus had the potential to eliminate air-conditioning. In terms of land area, these climates represented one-sixth (15.7%) of the world and were mainly concentrated in higher and lower latitudes. Between 2055 and 2085, the results suggest that as little as a 3.3% of people occupying 8.5% of the world's land area could live in climates where thermal mass and natural ventilation can eliminate air-conditioning (**Figures 9d** and **10d**). This represents a potential halving of the number of buildings that can be cooled by the simplest of passive means, on a per capita basis, globally.

It is also interesting to see where thermal mass could provide more than 50% of the cooling needs. Between 2055 and 2085, about three-quarters (71.8–77.9%) of the global population occupying two-thirds (60.7–69.5%) of the world's land area (**Figures 9b–d** and **10b–d**) will live in climates where thermal mass could still make such significant reductions to the SCL. Entire subcontinents such as the Sub-Saharan African regions, European as well as Eurasian regions, are shown to remain in these thermal mass-friendly climates, regardless of the RCP scenario considered, suggesting that thermal mass could still play a significant role in hybrid cooling approaches in the future, on a global scale.

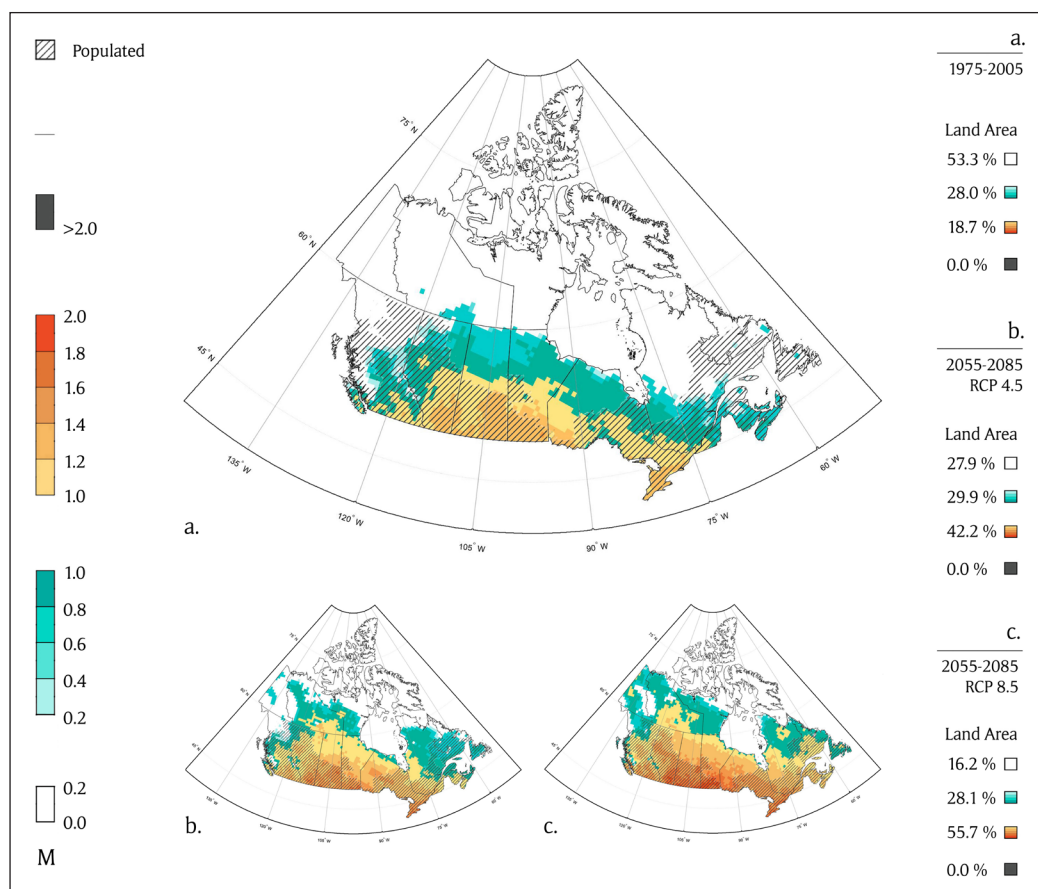


Figure 8: Thermal mass effectiveness levels for comfort in Canada during the hottest 30-day window for historical climate (a) and various future climates (b, c). ‘Unnecessary’ is indicated in white; ‘effective’ is indicated in the green scale; ‘partially effective’ is indicated in the amber scale; and ‘ineffective’ is indicated in grey.

Figure 9: Proportion of the world's land and population in regions where thermal mass is unnecessary (white), effective (green), partially effective (amber) and ineffective (grey), shown for current and future climates.



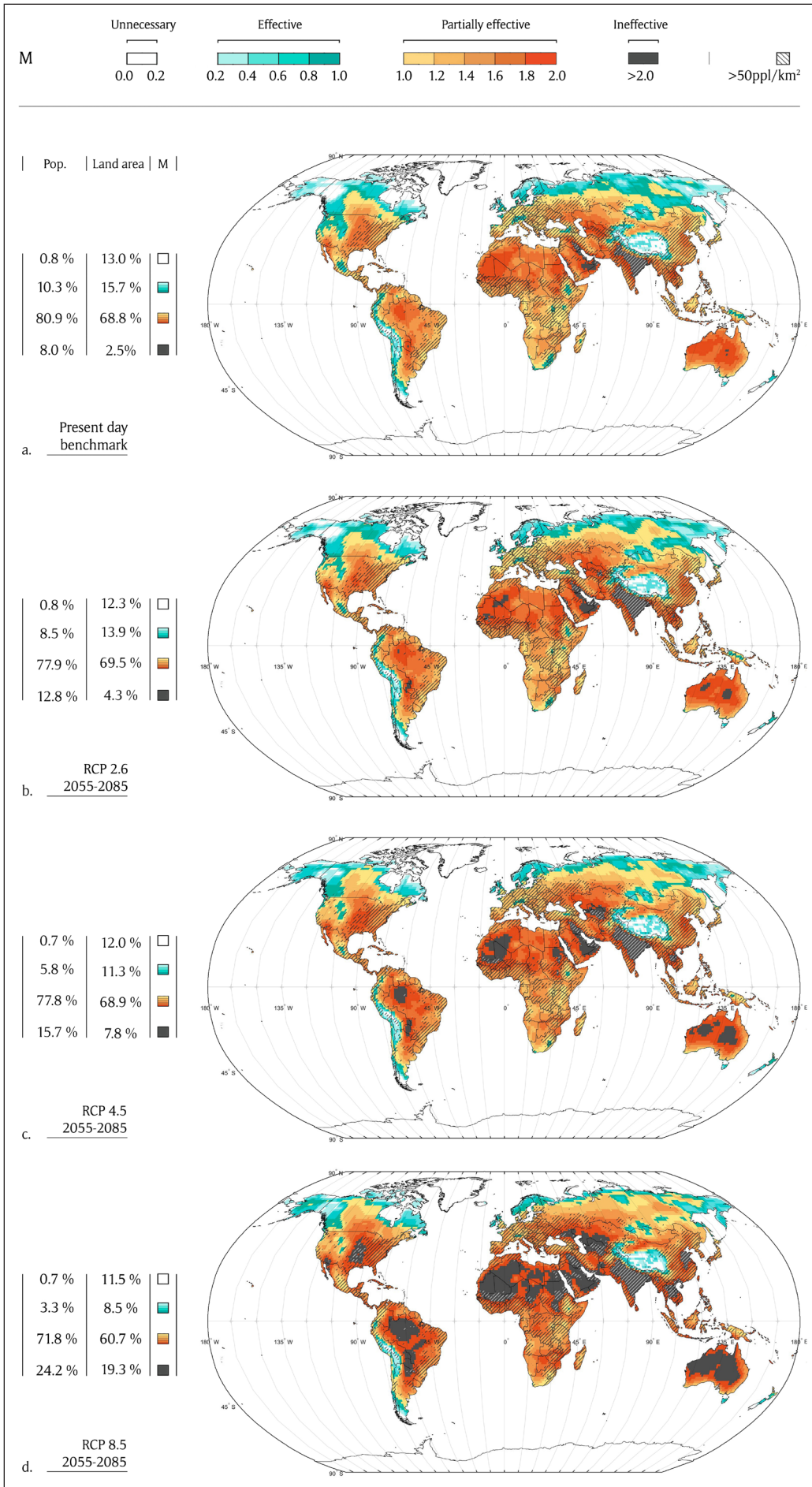


Figure 10: Thermal mass effectiveness levels for comfort during the hottest 30-day window for current and future climates. ‘Unnecessary’ is indicated in white; ‘effective’ is indicated in the green scale; ‘partially effective’ is indicated in the amber scale; and ‘ineffective’ is indicated in grey.

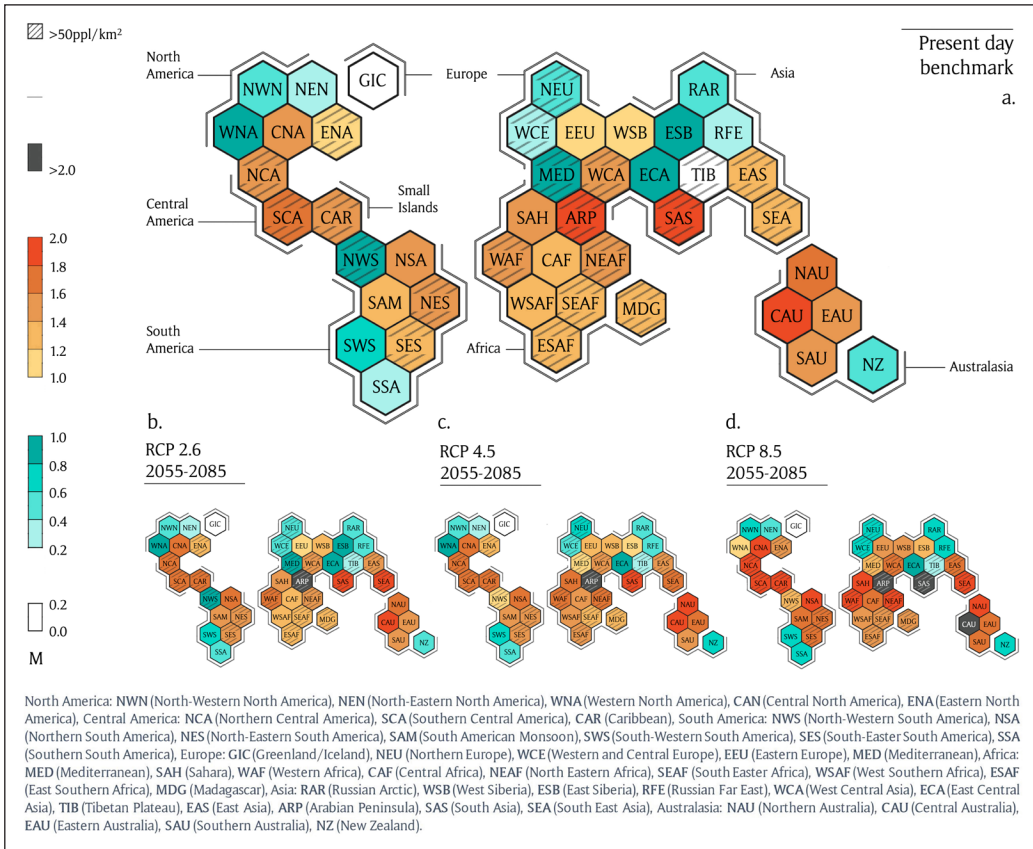


Figure 11: Thermal mass effectiveness levels for comfort during the hottest 30-day window for current and future climates, shown for AR6 reference regions (IPCC 2021). ‘Unnecessary’ is indicated in white; ‘effective’ is indicated in the green scale; ‘partially effective’ is indicated in the amber scale; and ‘ineffective’ is indicated in grey.

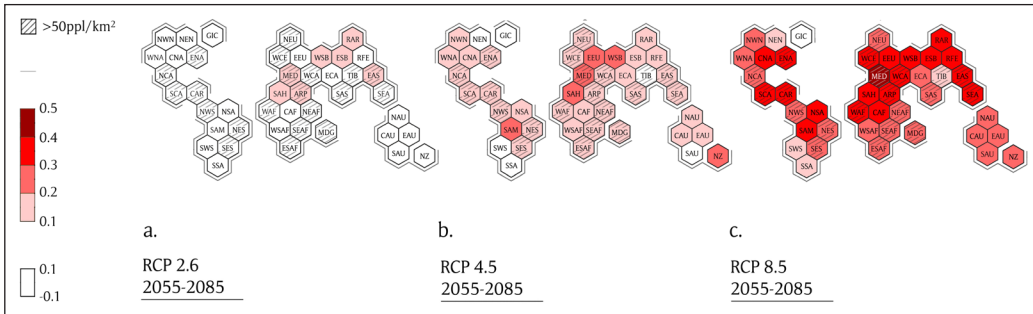
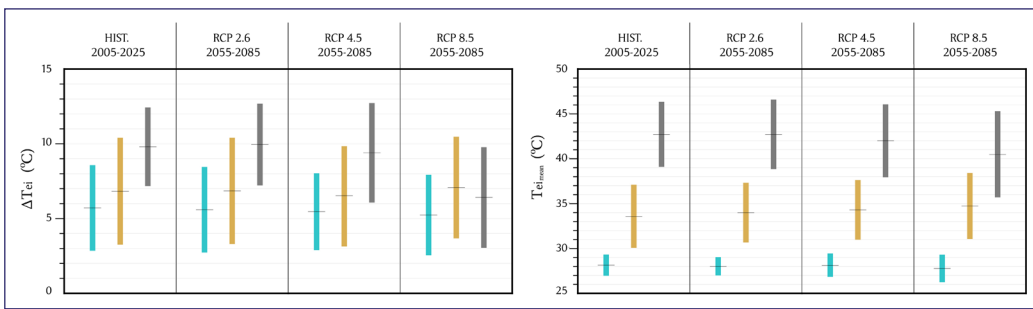


Figure 12: Relative change in the interior temperature damping required for comfort during the hottest 30 days between the present day baseline (2005-25) and future climates (RCP 2.4, 4.5 and 8.5 scenarios over the 2055-85 period).



Between 2055 and 2085, climates that render thermal mass ineffective (i.e. able to provide only less than half of the sensible cooling required) could grow sevenfold (+672.0%) to cover one-fifth of the world (19.3%) where up to one-quarter (24.20%) (versus 8.0% today) of the world’s population could live (**Figure 9a, d**). These climates would mainly span Southern Asia (SAS) and the Arabian Peninsula (ARP), Central Australia (CAU), as well as significant portions of West and Central Africa (WAF and SAH), Central Northern America (CNA) and Northern South America (NSA).

Figure 13: Average and standard deviation of the effective incoming air temperature mean ($Te_{i,\text{mean}}$) and increments above the mean (ΔTe_i) of the yearly 30 hottest days window for regions where thermal mass is effective (green), partially effective (amber) and ineffective (grey) from the multi-model mean of the global climate model (GCM) analysis.

Research has shown that cultural and other factors can influence what occupants deem comfortable in naturally ventilated buildings (Toe & Kubota 2013). Researchers have therefore undertaken to develop adjusted adaptive comfort thresholds suitable for different countries, especially those submitted to extreme temperatures. The authors comparatively computed the effectiveness of thermal mass over the Indian Peninsula using the Indian Model for Adaptive Comfort (IMAC) (Manu et al. 2016), but the results showed a negligible difference, suggesting that inter-adaptive comfort model variations are not significant enough to noticeably impact previsions of thermal mass usefulness during the hottest months.

Regions identified here as belonging to thermal mass-friendly climates should be the focus of further detailed RCM analyses to provide local actors of the building sector a detailed understanding of local thermal mass effectiveness levels.

4.2 IDEAL QUANTITIES

M	CONCRETE			MASS TIMBER			OSSB		
	S (M ²)	L (CM)	SF	S (M ²)	L (CM)	SF	S (M ²)	L (CM)	SF
0.2	0.45 ± 0.04	9.1 ± 1.1	1	0.93 ± 0.21	12.5 ± 3.1	3.75 ± 2.36	0.86 ± 0.05	13.9 ± 0.5	3.39 ± 1.19
0.3	0.98 ± 0.08	8.5 ± 1.0	1	2.00 ± 0.50	12.5 ± 3.1	3.92 ± 2.40	1.86 ± 0.16	13.9 ± 0.5	3.55 ± 1.38
0.4	1.85 ± 0.13	7.8 ± 0.9	1	3.70 ± 1.00	10.6 ± 1.1	3.30 ± 1.79	3.40 ± 0.40	12.8 ± 1.6	3.53 ± 1.69
0.5	3.32 ± 0.23	7.3 ± 0.9	1	6.50 ± 1.90	9.9 ± 0.5	3.20 ± 1.62	5.90 ± 0.50	11.4 ± 1.7	3.29 ± 1.49
0.6	6.00 ± 0.40	6.9 ± 0.8	1	11.50 ± 3.50	9.57 ± 0.42	3.16 ± 1.55	10.30 ± 0.90	9.9 ± 1.0	2.85 ± 1.12
0.7	11.30 ± 0.69	6.5 ± 0.8	1	22.00 ± 7.00	10.48 ± 1.3	3.98 ± 2.47	19.10 ± 1.60	9.2 ± 0.9	2.75 ± 1.05
0.8	26.60 ± 1.50	6.3 ± 0.8	1	47.00 ± 15.00	13.65 ± 4.8	5.97 ± 4.39	41.10 ± 3.40	8.8 ± 0.8	2.70 ± 1.03
0.9	81.00 ± 5.00	6.2 ± 0.8	1	154.00 ± 51.00	13.35 ± 4.6	6.05 ± 4.50	134.00 ± 11.00	8.6 ± 0.8	2.71 ± 1.02

The results demonstrate that massing proportions can compensate for inferior thermal properties. The concrete substitution factors for OSSB and mass timber (**Table 3**) suggest that biomass-based materials require on average 3.5 times the volume (V) of ceramic materials to perform equivalently.

A higher damping of interior conditions is shown to exponentially increase the required internally exposed surface (S) while proportionally moderately affecting the required thickness (l) (**Table 3**); more required cooling thus translates into greater material volumes to passively answer the demand. The required volumes of material are found to grow exponentially with each increment of temperature damping coefficient M (**Figure 15**), the exponential growth being directly proportional to the thermal properties of the materials (more acute for lower grade materials).

Figure 13 shows that the average daily effective incoming air temperature increments above the mean in thermal mass friendly climates is 6.35°C. This means that in these regions, one increment (0.1) of M translates to an interior temperature drop of 0.64°C, on average. **Figure 15** shows that, on average, the per capita required volumes of thermal mass material triple between damping coefficients of 0.8 and 0.9. This excessive increase in required material volume for < 1°C of additional cooling suggests that for high-temperature damping requirements (M > 0.8), reasonable practices should consider a practical material volume limit corresponding to that computed using M = 0.8 (**Figure 14a**).

When considering 3 m-wide floor space typologies with thermal mass exposed on one side of the room, the upper practical limit of interior temperature damping (M = 0.8) translates a per capita inhabited floor space of 24.6 ± 1.5 m² for concrete, 46.8 ± 15 m² for mass timber and 41.1 ± 3.4 m² for OSSB, thus showing that the use of thermal mass within low carbon building design practices does not fall far from recent low demand energy scenario proposing 30 m² per capita for decent living standards globally (Grubler et al. 2018).

Table 3: Per capita optimal internal thermal mass surfaces (S; m²), thicknesses (l; cm) and resulting concrete substitution factor (SF; dimensionless) for selected materials, shown for each increment of damping coefficient M.

Note: OSSB = oriented straw structural board.

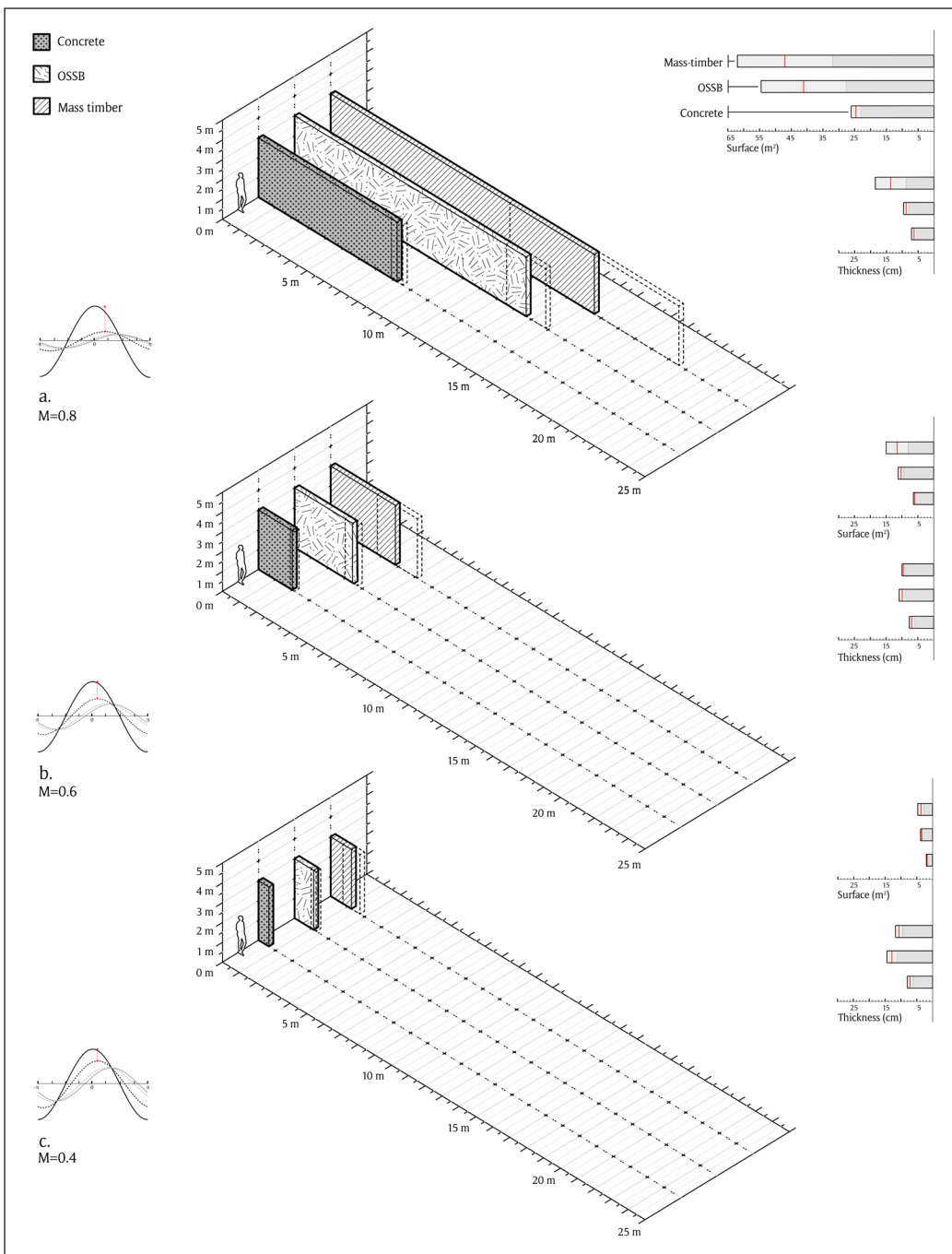


Figure 14: Per capita optimal thermal mass volume for high (a), medium (b) and low (c) required temperature damping. The surface and thickness of the thermal mass are indicated on the right-hand side.

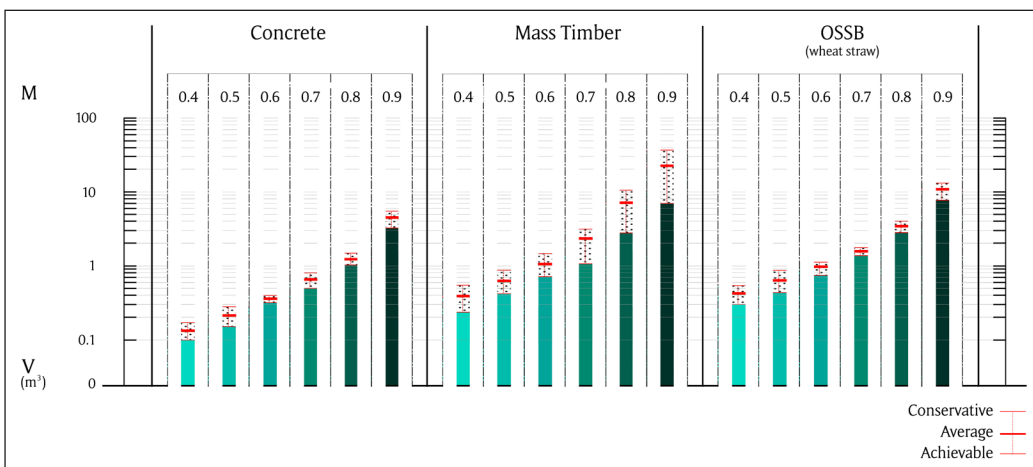


Figure 15: Per capita optimal volumes of material (V) for each increment of $M > 0.4$.

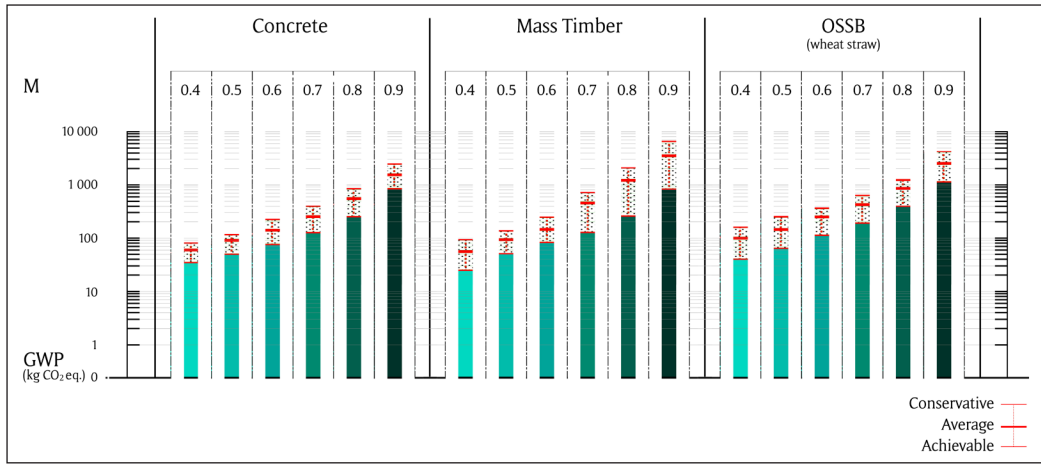


Figure 16: Conservative, average and achievable per capita embodied emissions (GWP; kg CO₂ eq.) shown for each increment of M > 0.4, computed using environmental product declarations (EPDs).

4.3 EMBODIED CARBON

With the comparison of the lifecycle carbon emissions of equivalently performing rather than strictly equivalent volumes of materials, the fair functional unit introduced in this study offers new insights into the outcomes of inter-material comparative LCA.

A traditional approach to comparative LCA using EPD data would systematically assume the embodied emissions of biogenic materials (i.e. an average of Canadian EPDs gives 135 ± 37 kg CO₂/m³ for mass timber and 229 ± 86 kg CO₂/m³ for OSSB) to be inferior to that of concrete (i.e. 374 ± 126 kg CO₂/m³) when comparing equivalent volumes of materials (i.e. for 1 m³, embodied emissions of concrete are respectively 2.7 and 1.6 times greater than that of mass timber and OSSB, respectively).

The comparison of the material's lifecycle carbon emissions carried out with the functional unit using EPD data (**Figure 16** and **Table 4**) shows that these trends are inverted; mass timber and OSSB embodied emissions are, on average (i.e. for each increment of M), 1.4 and 1.7 times greater than that of equivalently performing concrete volumes, respectively, which requires on average 3.5 times less material due to its higher thermal inertia (see Section 4.2 above).

Nevertheless, EPD data only cover the raw material supply, transport to the manufacturing site and manufacturing emissions, discarding, among others, carbon sequestered in biomass-based materials during the biomass growth over the year prior to construction (i.e. in the case of fast-rotation agricultural crop byproducts) or over previous decades (i.e. in the case of wood) or carbon subsequently sequestered by cementitious materials (i.e. carbonation of concrete). A sensitivity analysis performed considering yearly carbon absorption rates for a 100-year time horizon following standard carbonation kinetics (NIC 2006) and dynamic LCA (Levasseur et al. 2013) (i.e. using the 'optimal' per person thickness and surface of concrete internally exposed to air to compute, for each damping coefficient increment, the carbonation rate and carbonation potential of the internal thermal mass) shows, for instance, that carbonation uptakes could reduce concrete emissions by an average of 19% for each increment of M. How and whether or not to include dynamic assessment of concrete carbonation uptakes, biogenic carbon sequestration and other parameters (e.g. negative land-use emissions from sustainable forestry practices; Head et al. 2019, 2020) for product comparison are highly controversial issues (Arehart et al. 2021; Collins 2010; TFD 2021) which are beyond the scope of this paper. As the temporal and spatial system boundaries chosen for inter-material comparative analyses remain of critical importance (Hoxha et al. 2020), the functional unit should be used by design teams to perform informed assessments with exhaustive emission data covering the various material life-stages and processes contextually considered of significant importance (e.g. the analysis performed here misrepresents the considerable opportunity provided by materials such as OSSB made from otherwise burnt straw byproducts of the agro-industrial sector to momentarily store biogenic carbon in the building stock; Göswein et al. 2021).

Simplifying material assemblies through good thermal mass design enables an easier accounting and more reliable predictions of a building's embodied emissions, as well as an easier agency in sourcing the primary materials. Yet, the study should not be understood as consistently advocating for the use of less material to lower the embodied emissions of the material assemblies—meaning, on an absolute basis, less available volume for carbon sequestration. In the Canadian framework of abundant supplies of agricultural byproducts and sustainably sourced HWPs, the sequestration potential of the building stock should be skillfully maximized through an optimal balance between feasible construction/retrofitting rates, material supplies and inter-sector competition. Complex risk assessments (Simpson et al. 2021) should be conducted to expose the non-linear nature of policies' potential outcomes on the national scale, e.g. falling concrete prices due to reduced market opportunities might counterproductively induce increased use elsewhere, possibly requiring the artificial maintenance of market prices (Harmon 2019); or timber rising prices due to increased demand might have unforeseen impacts on forests land-use change (Lubowski et al. 2008).

M	CONCRETE	MASS TIMBER	OSSB
	GWP (KG CO ₂ EQ.)	GWP (KG CO ₂ EQ.)	GWP (KG CO ₂ EQ.)
0.2	14.83 ± 7.70	18.33 ± 12.18	27.82 ± 13.59
0.3	28.83 ± 15.29	38.96 ± 26.10	59.50 ± 31.45
0.4	51.97 ± 26.32	57.35 ± 34.15	105.62 ± 64.29
0.5	86.78 ± 44.00	92.50 ± 52.10	163.65 ± 96.23
0.6	146.86 ± 72.58	157.06 ± 87.98	241.69 ± 132.43
0.7	263.85 ± 132.14	355.59 ± 239.14	414.73 ± 221.36
0.8	554.95 ± 280.24	1125.68 ± 867.80	850.12 ± 449.78
0.8	1767.37 ± 898.62	3,609.05 ± 2,804.16	2,701.48 ± 1,412.99

Table 4: Per capita embodied emissions (GWP; kg CO₂ eq.) for each increment of M.

Note: OSSB = oriented straw structural board.

5. CONCLUSIONS

Through its ability to reduce the material requirements of buildings to their strict useful minimum; to integrate several functions into a main mono-material assembly (i.e. regulating temperature, ventilation and structure); and to sequester biogenic carbon in the building stock (biogenic materials are suitable material candidates), optimally scaled naturally ventilated internal thermal mass can participate in turning the existing and growing building stock into a powerful climate change mitigating strategy.

Climate data are used to identify region types based on the local effectiveness of naturally ventilated internal thermal mass to mitigate current and future heatwaves, ranging from places where air-conditioning use can entirely be obviated to places where entirely different cooling strategies are necessary.

A high-resolution climate analysis performed over Canada shows that wherever cooling will be necessary in future climates, internal thermal mass can cut sensible cooling loads (SCL) by more than 50% and could thus play a significant role in hybrid cooling approaches.

The methodology developed could be applied to other regions, and lower resolution indicative results of the effectiveness of internal thermal mass on a global scale are given so that subsequent studies can focus on regions identified as having a high applicability potential.

Results show that in the near future (2055–85), as little as 3.3% of the world population, occupying one-tenth (8.5%) of the world land area (mainly concentrated in higher and lower latitudes), will live in climates where internal thermal mass and natural ventilation can entirely eliminate air-conditioning, thus limiting the number of buildings that can be cooled through the simplest of passive means, on a per capita basis, globally. Climates where internal thermal mass is ineffective could grow sevenfold (+672.0%) to cover one-fifth of the world (19.3%), where up to 24.2% (versus

8.0% today) of the world's population could live, mainly spanning Southern Asia (SAS) and the Arabian Peninsula (ARP), Central Australia (CAU), as well as significant portions of West and Central Africa (WAF and SAH), Central Northern America (CNA) and Northern South America (NSA). Regions where internal thermal mass is found to be or become ineffective are thus found to intersect with population centers confronted to both the lowest human development indexes (UNDP 2020) and the highest share of people with no access to electricity (WBG 2019)—204.89 million people in India alone. The ability of good internal thermal mass design to address the global patterns of heat-stress inequalities which are exacerbated by the climate crisis is thus shown to be limited. Yet, two-thirds of the world's land area (60.7–69.5%)—including entire subcontinents such as Sub-Saharan African regions, European as well as Eurasian regions—occupied by three-quarters (71.8–77.9%) of the global population is shown to remain in climates where internal thermal mass could cut the per capita SCL by more than half, suggesting that naturally ventilated internal thermal mass could nevertheless also, at the global scale, play a significant role in hybrid cooling approaches. Further studies should enquire about the ability of recently developed passive cooling technologies (e.g. sky radiative cooling; Zhou et al. 2019) to be coupled to the work of internal thermal mass and harnessed to lower the interior diurnal temperature cycles enough to passively provide thermal comfort where thermal mass alone is insufficient.

In thermal mass-friendly climates, the necessary thermal mass quantities required to provide sufficient thermal comfort and ventilation during the hottest month without mechanical assistance are estimated for each region, on a per capita basis, showing that biomass-based materials require on average 3.5 times the volume of cementitious materials for equivalent thermodynamic performance. The results suggest that the per person material volumes required to be positioned by design teams inside inhabited floor spaces to harness the maximum potential for internal thermal mass work (i.e. providing high-temperature damping and necessary per person ventilation rates) remain reasonable and similar to dimensions used in construction (\approx 6.3 cm-thick thermal mass with an interior surface area of 26.6 m² for concrete, 13.6 cm thick and 47.0 m² for mass timber, and 8.8 cm thick and 41.1 m² for oriented straw structural boards—OSSB). Based on these findings, concrete substitution factors are developed for biomass-based materials.

Finally, an analysis of the embodied carbon emissions of per capita optimal thermal mass quantities is performed, suggesting that the latter could be used as a fair functional unit for inter-material comparative lifecycle assessments (LCAs) in low-carbon building design to allow a comparison of the environmental impact of equivalently performing, rather than equivalent volumes of materials.

AUTHOR AFFILIATIONS

Timothée de Toldi  orcid.org/0000-0002-2959-3490

Civil Engineering, McGill University, Montreal, QC, Canada

Salmaan Craig  orcid.org/0000-0001-7830-2752

Peter Guo-hua Fu School of Architecture, McGill University, Montreal, QC, Canada

Laxmi Sushama  orcid.org/0000-0002-0852-1009

Civil Engineering, McGill University, Montreal, QC, Canada

COMPETING INTERESTS

The authors declare that they have no known competing financial interests or personal relationships that could have appeared to influence the work reported in this paper.

ETHICAL APPROVAL

Ethics approval was not required for this research.

FUNDING

This research was supported by the McGill Sustainability Systems Initiative (MSSI).

Supplemental data files for this article can be accessed at: <https://doi.org/10.5334/bc.156.s1>.

de Toldi et al.
Buildings and Cities
DOI: 10.5334/bc.156

REFERENCES

- Addis, W.** (2007). *Building: 3000 years of design engineering and construction*. Phaidon. <http://swbplus.bsz-bw.de/bsz264712781inh.pdf>
- ADEME & IGN.** (2019). *Contribution de l'IGN à l'établissement des bilans carbone des forêts des territoires (PCAET)*. Agence de l'Environnement et de la Maîtrise de l'Energie (ADEME) and Institut Géographique National (IGN). <https://www.territoires-climat.ademe.fr/Uploads/media/default/0001/01/02555bb8e15c98da373799a510ae5561aaadb2b0.pdf>
- ANSI/ASHRAE.** (2017). *Standard 55: Thermal environmental conditions for human occupancy*.
- Arehart, J. H., Hart, J., Pomponi, F., & D'Amico, B.** (2021). Carbon sequestration and storage in the built environment. *Sustainable Production and Consumption*, 27, 1047–1063. DOI: <https://doi.org/10.1016/j.spcl.2021.02.028>
- Ashby, M. F.** (2011). *Materials selection in mechanical design*, 4th ed. Butterworth-Heinemann. <http://www.dawsonera.com/depp/reader/protected/external/AbstractView/S9780080952239>
- Ashby, M. F.** (2013). *Materials and the environment: Eco-informed material choice*. Butterworth-Heinemann. DOI: <https://doi.org/10.1016/B978-0-12-385971-6.00010-5>
- ASHRAE.** (2013). *ASHRAE handbook: Fundamentals* (SI ed.). American Society of Heating, Refrigerating and Air-Conditioning Engineers (ASHRAE). <http://app.knovel.com/hotlink/toc/id:kpASHRAEC1/2013-ashrae-handbook>
- Barrett, L., Jeong, J., Price, R., Subasic, C., Asselin, S., Fortin, R., Freear, A., Kennedy, D., Moe, K., & Craig, S.** (2021). Synchronized coupling of thermal mass and buoyancy ventilation: Wood versus concrete. *Journal of Physics: Conference Series*, 2042(1), 012152. DOI: <https://doi.org/10.1088/1742-6596/2042/1/012152>
- Berardi, U., & Jafarpur, P.** (2020). Assessing the impact of climate change on building heating and cooling energy demand in Canada. *Renewable and Sustainable Energy Reviews*, 121, 109681. DOI: <https://doi.org/10.1016/j.rser.2019.109681>
- Brager, G., Zhang, H., & Arens, E.** (2015). Evolving opportunities for providing thermal comfort. *Building Research & Information*, 43(3), 274–287. DOI: <https://doi.org/10.1080/09613218.2015.993536>
- Carlisle, S., Waldman, B., Lewis, M., & Simonen, K.** (2021). Carbon Leadership Forum material baseline report. Paper presented at the Carbon Leadership Forum, University of Washington. Seattle, WA. <https://carbonleadershipforum.org/material-baselines/>
- CEN.** (2011). EN-15804. In *Sustainability of construction works—Assessment of environmental performance of buildings—Calculation method*. Comité Européen de Normalisation (CEN). <https://standards.globalspec.com/std/1666865/en-15804>
- Cheng, W., Han, G., & Fang, D.** (2013). Oriented structural boards from split wheat straw: Effects of straw length, panel density, and resin content. *BioResources*, 8(3), 4497–4504. DOI: <https://doi.org/10.15376/biores.8.3.4497-4504>
- Cole, R. J., Robinson, J., Brown, Z., & O'Shea, M.** (2008). Re-contextualizing the notion of comfort. *Building Research & Information*, 36(4), 323–336. DOI: <https://doi.org/10.1080/09613210802076328>
- Collins, F.** (2010). Inclusion of carbonation during the life cycle of built and recycled concrete: Influence on their carbon footprint. *International Journal of Life Cycle Assessment*, 15(6), 549–556. DOI: <https://doi.org/10.1007/s11367-010-0191-4>
- Cordier, S., Robichaud, F., Blanchet, P., & Amor, B.** (2021). Regional environmental life cycle consequences of material substitutions: The case of increasing wood structures for non-residential buildings. *Journal of Cleaner Production*, 328, 129671. DOI: <https://doi.org/10.1016/j.jclepro.2021.129671>
- Côté, J., Gravel, S., Méthot, A., Patoine, A., Roch, M., & Staniforth, A.** (1998). The Operational CMC-MRB Global Environmental Multiscale (GEM) Model. Part I: Design considerations and formulation. *Monthly Weather Review*, 126(6), 1373–1395. DOI: [https://doi.org/10.1175/1520-0493\(1998\)126<1373:TOCMGE>2.0.CO;2](https://doi.org/10.1175/1520-0493(1998)126<1373:TOCMGE>2.0.CO;2)
- Craig, S.** (2019). The optimal tuning, within carbon limits, of thermal mass in naturally ventilated buildings. *Building and Environment*, 165. DOI: <https://doi.org/10.1016/j.buildenv.2019.106373>
- De Wolf, C., Pomponi, F., & Moncaster, A.** (2017). Measuring embodied carbon dioxide equivalent of buildings: A review and critique of current industry practice. *Energy & Buildings*, 140, 68–80. DOI: <https://doi.org/10.1016/j.enbuild.2017.01.075>
- Drever, C. R., Cook-Patton, S. C., Akhter, F., Badiou, P. H., Chmura, G. L., Davidson, S. J., Desjardins, R. L., Dyk, A., Fargione, J. E., Fellows, M., Filewod, B., Hessing-Lewis, M., Jayasundara, S., Keeton, W. S.,**

- Kroeger, T., Lark, T. J., Le, E., Leavitt, S. M., LeClerc, M.-E., Lemière, T. C., Metsaranta, J., McConkey, B., Neilson, E., St-Laurent, G. P., Puric-Mladenovic, D., Rodrigue, S., Soolanayakanahally, R. Y., Spawn, S. A., Strack, M., Smyth, C., Thevathasan, N., Voicu, M., Williams, C. A., Woodbury, P. B., Worth, D. E., Xu, Z., Yeo, S., & Kurz, W. A. (2021). Natural climate solutions for Canada. *Science Advances*, 7(23), eabd6034. DOI: <https://doi.org/10.1126/sciadv.abd6034>
- EC3.** (2020). *Embodied carbon in construction calculator (EC3)*. Building Transparency. <https://buildingtransparency.org/ec3>
- ECCC.** (2018–21). *Climate data for a resilient Canada: Data download*. Environment and Climate Change Canada (ECCC). <https://climatedata.ca/download/>
- ECCC.** (2021). *Weather summaries*. Environment and Climate Change Canada (ECCC). https://weather.gc.ca/warnings/weathersummaries_e.html
- Göswein, V., Silvestre, J. D., Sousa Monteiro, C., Habert, G., Freire, F., & Pittau, F. (2021). Influence of material choice, renovation rate, and electricity grid to achieve a Paris Agreement-compatible building stock: A Portuguese case study. *Building and Environment*, 195, 107773. DOI: <https://doi.org/10.1016/j.buildenv.2021.107773>
- Government of Canada.** (2021). *The ensemble of daily predictor variables developed from the CanESM2 CMIP5 experiments*. <https://climate-scenarios.canada.ca/?page=canesm2-predictor-notes>
- Grubler, A., Wilson, C., Bento, N. et al. (2018). A low energy demand scenario for meeting the 1.5°C target and sustainable development goals without negative emission technologies. *Nature Energy*, 3, 515–527. DOI: <https://doi.org/10.1038/s41560-018-0172-6>
- Habert, G., Röck, M., Steininger, K., Lupísek, A., Birgisdottir, H., Desing, H., Chandrakumar, C., Pittau, F., Passer, A., Rovers, R., Slavkovic, K., Hollberg, A., Hoxha, E., Jusselme, T., Nault, E., Allacker, K., & Lützkendorf, T. (2020). Carbon budgets for buildings: Harmonising temporal, spatial and sectoral dimensions. *Buildings and Cities*, 1(1), 429–452. DOI: <https://doi.org/10.5334/bc.47>
- Harmon, M. E. (2019). Have product substitution carbon benefits been overestimated? A sensitivity analysis of key assumptions. *Environmental Research Letters*, 14(6), 065008. DOI: <https://doi.org/10.1088/1748-9326/ab1e95>
- Head, M., Bernier, P., Levasseur, A., Beauregard, R., & Margni, M. (2019). Forestry carbon budget models to improve biogenic carbon accounting in life cycle assessment. *Journal of Cleaner Production*, 213, 289–299. DOI: <https://doi.org/10.1016/j.jclepro.2018.12.122>
- Head, M., Levasseur, A., Beauregard, R., & Margni, M. (2020). Dynamic greenhouse gas life cycle inventory and impact profiles of wood used in Canadian buildings. *Building and Environment*, 173, 106751. DOI: <https://doi.org/10.1016/j.buildenv.2020.106751>
- Holford, J. M., & Woods, A. W. (2007). On the thermal buffering of naturally ventilated buildings through internal thermal mass. *Journal of Fluid Mechanics*, 580, 3–29. DOI: <https://doi.org/10.1017/S0022112007005320>
- Hoxha, E., Passer, A., Saade, M. R. M., Trigaux, D., Shuttleworth, A., Pittau, F., Allacker, K., & Habert, G. (2020). Biogenic carbon in buildings: A critical overview of LCA methods. *Buildings and Cities*, 1(1), 504–524. DOI: <https://doi.org/10.5334/bc.46>
- IEA.** (2018). *The Future of Cooling*. International Energy Agency (IEA). <https://www.iea.org/reports/the-future-of-cooling>
- Igaz, R., Kristak, L., Ruziak, I., Gajtanska, M., & Kucerka, M. (2017). Thermophysical properties of OSB boards versus equilibrium moisture content. *BioResources*, 12(4), 8106–8118. DOI: <https://doi.org/10.15376/biores.12.4.8106-8118>
- IPCC.** (2021). Climate change 2021: The physical science basis. *Contribution of Working Group I to the Sixth Assessment Report of the Intergovernmental Panel on Climate Change* (eds.) Masson-Delmotte, V., P. Zhai, A. Pirani, S. L. Connors, C. Péan, S. Berger, N. Caud, Y. Chen, L. Goldfarb, M. I. Gomis, M. Huang, K. Leitzell, E. Lonnoy, J. B. R. Matthews, T. K. Maycock, T. Waterfield, O. Yelekçi, R. Yu & B. Zhou]. Cambridge University Press.
- Jones, B., & O'Neill, B. C. (2016). Spatially explicit global population scenarios consistent with the shared socioeconomic pathways. *Environmental Research Letters*, 11(8), 084003. DOI: <https://doi.org/10.1088/1748-9326/11/8/084003>
- Khosla, R., Miranda, N. D., Trotter, P. A., Mazzone, A., Renaldi, R., McElroy, C., Cohen, F., Jani, A., Perera-Salazar, R., & McCulloch, M. (2021). Cooling for sustainable development. *Nature Sustainability*, 4(3), 201–208. DOI: <https://doi.org/10.1038/s41893-020-00627-w>
- Khvalyag, D., Kazancı, O. B., Halvorsen, H., Gundlach, I., Bahnfleth, W. P., Toftum, J., & Olesen, B. W. (2020). Critical review of standards for indoor thermal environment and air quality. *Energy and Buildings*, 213, 109819. DOI: <https://doi.org/10.1016/j.enbuild.2020.109819>

- Knutti, R., Masson, D., & Gettelman, A.** (2013). Climate model genealogy: Generation CMIP5 and how we got there. *Geophysical Research Letters*, 40(6), 1194–1199. DOI: <https://doi.org/10.1002/grl.50256>
- Lee, M., Jun, M., & Genton, M. G.** (2015). Validation of CMIP5 multimodel ensembles through the smoothness of climate variables. *Tellus A: Dynamic Meteorology and Oceanography*, 67(1), 23880. DOI: <https://doi.org/10.3402/tellusa.v67.23880>
- Levasseur, A., Lesage, P., Margni, M., & Samson, R.** (2013). Biogenic carbon and temporary storage addressed with dynamic life cycle assessment. *Journal of Industrial Ecology*, 17(1), 117–128. DOI: <https://doi.org/10.1111/j.1530-9290.2012.00503.x>
- Lishman, B., & Woods, A. W.** (2009). The effect of gradual changes in wind speed or heat load on natural ventilation in a thermally massive building. *Building and Environment*, 44, 762–772. DOI: <https://doi.org/10.1016/j.buildenv.2008.06.026>
- Lubowski, R. N., Plantinga, A. J., & Stavins, R. N.** (2008). What drives land-use change in the United States? A national analysis of landowner decisions. *Land Economics*, 84, 529–550. <http://web.ebscohost.com.ezproxy1.hul.harvard.edu/ehost/detail?vid=4&hid=15&sid=a6b20f94-e58f-496c-8472-5d1af9835f9e40sesionmgr15&bdata=JnNpdGU9ZWhvc3QtbG12ZSzY29wZT1zaXRl#db=bth&AN=34589788>
- Lützkendorf, T.** (2020). The role of carbon metrics in supporting built-environment professionals. *Buildings and Cities*, 1(1), 676–686. DOI: <https://doi.org/10.5334/bc.73>
- Manu, S., Shukla, Y., Rawal, R., Thomas, L. E., & de Dear, R.** (2016). Field studies of thermal comfort across multiple climate zones for the subcontinent: India Model for Adaptive Comfort (IMAC). *Building and Environment*, 98, 55–70. DOI: <https://doi.org/10.1016/j.buildenv.2015.12.019>
- Meinshausen, M., Nicholls, Z. R. J., Lewis, J., Gidden, M. J., Vogel, E., Freund, M., Beyerle, U., Gessner, C., Nauels, A., Bauer, N., Canadell, J. G., Daniel, J. S., John, A., Krummel, P. B., Luderer, G., Meinshausen, N., Montzka, S. A., Rayner, P. J., Reimann, S., Smith, S. J., van den Berg, M., Velders, G. J. M., Vollmer, M. K., & Wang, R. H. J.** (2020). The shared socio-economic pathway (SSP) greenhouse gas concentrations and their extensions to 2500. *Geoscientific Model Development*, 13(8), 3571–3605. DOI: <https://doi.org/10.5194/gmd-13-3571-2020>
- Moazami, A., Nik, V. M., Carlucci, S., & Geving, S.** (2019). Impacts of future weather data typology on building energy performance—Investigating long-term patterns of climate change and extreme weather conditions. *Applied Energy*, 238, 696–720. DOI: <https://doi.org/10.1016/j.apenergy.2019.01.085>
- Moncaster, A. M., Pomponi, F., Symons, K. E., & Guthrie, P. M.** (2018). Why method matters: Temporal, spatial and physical variations in LCA and their impact on choice of structural system. *Energy & Buildings*, 173, 389–398. DOI: <https://doi.org/10.1016/j.enbuild.2018.05.039>
- Nellis, G., & Klein, S. A.** (2009). Heat transfer. Cambridge University Press. <http://catdir.loc.gov/catdir/toc/ecip0818/2008021961.html>
- NIC.** (2006). Carbon dioxide uptake during concrete life cycle—State of the art. https://www.dti.dk/_media/21043_769417_Task%201_final%20report_CBI_Bjorn%20Lagerblad.pdf
- Nicol, F.** (2006). Standards for thermal comfort: Indoor air temperature standards for the 21st century. Taylor & Francis. <http://search.ebscohost.com/login.aspx?direct=true&scope=site&db=nlebk&db=nlabk&AN=1131845>
- Nicol, F., Humphreys, M. A., & Roaf, S.** (2012). Adaptive thermal comfort: principles and practice. Routledge. DOI: <https://doi.org/10.4324/9780203123010>
- NRC.** (2010). National building code of Canada, 2010. National Research Council of Canada (NRC), Institute for Research in Construction.
- Pomponi, F., & Moncaster, A.** (2016). Embodied carbon mitigation and reduction in the built environment—What does the evidence say? *Journal of Environmental Management*, 181, 687–700. DOI: <https://doi.org/10.1016/j.jenvman.2016.08.036>
- Pomponi, F., Moncaster, A., & De Wolf, C.** (2018). Furthering embodied carbon assessment in practice: Results of an industry-academia collaborative research project. *Energy and Buildings*, 167, 177–186. DOI: <https://doi.org/10.1016/j.enbuild.2018.02.052>
- Pomponi, F., Piroozfar, P. A. E., & Farr, E. R. P.** (2016). An investigation into GHG and non-GHG impacts of double skin façades in office refurbishments. *Journal of Industrial Ecology*, 20(2), 234–248. DOI: <https://doi.org/10.1111/jiec.12368>
- PPG & TCIC.** (2008). Straw procurement business case. Prairie Practitioners Group (PPG) & The Composites Innovation Centre (TCIC). <https://www.gov.mb.ca/agriculture/innovation-and-research/pubs/straw-procurement-final-report.pdf>
- Roberge, F., & Sushama, L.** (2018). Urban heat island in current and future climates for the island of Montreal. *Sustainable Cities and Society*, 40, 501–512. DOI: <https://doi.org/10.1016/j.scs.2018.04.033>
- Röck, M., Saade, M. R. M., Balouktsi, M., Rasmussen, F. N., Birgisdottir, H., Frischknecht, R., Habert, G., Lützkendorf, T., & Passer, A.** (2020). Embodied GHG emissions of buildings—The hidden challenge for effective climate change mitigation. *Applied Energy*, 258, 114107. DOI: <https://doi.org/10.1016/j.apenergy.2019.114107>

- Sadeghi, M., De Dear, R., Morgan, G., Santamouris, M., & Jalaludin, B.** (2021). Development of a heat stress exposure metric—Impact of intensity and duration of exposure to heat on physiological thermal regulation. *Building and Environment*, 200, 107947. DOI: <https://doi.org/10.1016/j.buildenv.2021.107947>
- Sherwood, S. C., & Huber, M.** (2010). An adaptability limit to climate change due to heat stress. *Proceedings of the National Academy of Sciences*, 107(21), 9552–9555. DOI: <https://doi.org/10.1073/pnas.0913352107>
- Simpson, N. P., Mach, K. J., Constable, A., Hess, J., Hogarth, R., Howden, M., Lawrence, J., Lempert, R. J., Muccione, V., Mackey, B., New, M. G., O'Neill, B., Otto, F., Pörtner, H.-O., Reisinger, A., Roberts, D., Schmidt, D. N., Seneviratne, S., Strongin, S., Van Aalst, M., Totin, E., & Trisos, C. H.** (2021). A framework for complex climate change risk assessment. *One Earth*, 4(4), 489–501. DOI: <https://doi.org/10.1016/j.oneear.2021.03.005>
- Statistics Canada.** (2018). Forest management greenhouse gas inventory. <https://cfs.nrcan.gc.ca/statsprofile/>
- Statistics Canada.** (2021). Estimated areas, yield, production, average farm price and total farm value of principal field crops, in metric and imperial units. <https://doi.org/10.25318/3210035901-eng>
- Tabarsa, T., Jahanshahi, S., & Ashori, A.** (2011). Mechanical and physical properties of wheat straw boards bonded with a tannin modified phenol-formaldehyde adhesive. *Composites Part B: Engineering*, 42(2), 176–180. DOI: <https://doi.org/10.1016/j.compositesb.2010.09.012>
- Teufel, B., & Sushama, L.** (2019). Abrupt changes across the Arctic permafrost region endanger northern development. *Nature Climate Change*, 9(11), 858–862. DOI: <https://doi.org/10.1038/s41558-019-0614-6>
- TFD.** (2021). *Climate benefits and challenges related to ‘mass timber’ construction: From frame to forest*. The Forest Dialogue (TFD).
- Toe, D. H. C., & Kubota, T.** (2013). Development of an adaptive thermal comfort equation for naturally ventilated buildings in hot-humid climates using ASHRAE RP-884 database. *Frontiers of Architectural Research*, 2(3), 278–291. DOI: <https://doi.org/10.1016/j foar.2013.06.003>
- UNDP.** (2020). *Human development report*. United Nations Development Programme (UNDP). <http://hdr.undp.org/en/data>
- Waldman, B., Huang, M., & Simonen, K.** (2020). Embodied carbon in construction materials: A framework for quantifying data quality in EPDs. *Buildings and Cities*, 1(1), 625–636. DOI: <https://doi.org/10.5334/bc.31>
- WBG.** (2019). *World development indicators*. World Bank Group (WGB). <https://datacatalog.worldbank.org/dataset/world-development-indicators>
- Yassaghi, H., & Hoque, S.** (2019). An overview of climate change and building energy: Performance, responses and uncertainties. *Buildings*, 9(7), 166. DOI: <https://doi.org/10.3390/buildings9070166>
- Zhou, L., Song, H., Liang, J., Singer, M., Zhou, M., Stegenburgs, E., Zhang, N., Xu, C., Ng, T., Yu, Z., Ooi, B., & Gan, Q.** (2019). A polydimethylsiloxane-coated metal structure for all-day radiative cooling. *Nature Sustainability*, 2(8), 718–724. DOI: <https://doi.org/10.1038/s41893-019-0348-5>

de Toldi et al.
Buildings and Cities
DOI: 10.5334/bc.156

TO CITE THIS ARTICLE:
De Toldi, T., Craig, S., & Sushama, L. (2022). Internal thermal mass for passive cooling and ventilation: adaptive comfort limits, ideal quantities, embodied carbon. *Buildings and Cities*, 3(1), pp. 42–67. DOI: <https://doi.org/10.5334/bc.156>

Submitted: 12 September 2021
Accepted: 01 February 2022
Published: 02 March 2022

COPYRIGHT:
© 2022 The Author(s). This is an open-access article distributed under the terms of the Creative Commons Attribution 4.0 International License (CC-BY 4.0), which permits unrestricted use, distribution, and reproduction in any medium, provided the original author and source are credited. See <http://creativecommons.org/licenses/by/4.0/>.

Buildings and Cities is a peer-reviewed open access journal published by Ubiquity Press.